Intraspecific adaptive response of *Periconia macrospinosa*, a ubiquitous root-associated fungus, to persistent salinity stress provides evidence for its adaptive variability and high-osmolarity glycerol pathway mediated adaptive response

by

Kyle Joseph Ismert

B.S., Kansas State University, 2018

A THESIS

submitted in partial fulfillment of the requirements for the degree

MASTER OF SCIENCE

Division of Biology
College of Arts and Sciences

KANSAS STATE UNIVERSITY
Manhattan, Kansas

2022

Approved by:
Major Professor
Ari Jumpponen

Copyright

Abstract

Root associated fungi are critical to environmental success of their plant hosts. Whether through their interactions with hosts, nutrient recycling, decomposition, or even contribution to soil structure, soil-dwelling fungi play a pivotal role in environmental preservation and function. As climate change continues to affect and change patterns in climate, researchers are increasingly concerned about the impacts our global environments may endure as a result. In a terrestrial ecosystem, mean annual precipitation (MAP) is an important control of biological productivity. As water leaves a system, via evapotranspiration, mass flow, surface flow, or other means, salts remain and concentrate in soils causing salinity stress for organisms that remain. This increasing salt concentration is a major stressor for organisms and requires specialized osmoadaptive responses. Plant communities as well as those of soil-dwelling fungi and bacteria change along precipitation gradients, indicating their responses to water availability. However, it is less certain if conspecific organisms also differ across similar gradients, especially in their abilities to tolerate salt stress.

To investigate the inter- and intraspecific adaptive responses of root-associated ascomycetes to salinity, we devised an experiment wherein conspecific isolates representing five ascomycete species were subjected to increasing concentrations of salinity in an effort to quantify and compare the effective dose of salt (NaCl) necessary to limit colony growth by 50% (ED_{50}). For each of the five species, we selected three conspecifics originating from drier "arid" environments and compared those to three conspecifics originating from wetter "mesic" environments. We hypothesized that (1) ascomycete species differ in their growth response to salinity across species; (2) conspecific strains from drier sites have greater salt tolerance than those from more mesic sites. Each isolate was tested three times in triplicate and exposed to four

levels of NaCl concentrations in a quad-plate. We measured colony growth and used regression analyses to estimate the isolates' ED_{50}. In support of our first hypothesis, we observed that species differed in their growth response to salinity according to ED_{50}. However, we observed no consistent, strong evidence to support our second hypothesis. Still, we observed non-significant differences in ED_{50} within three species observed, partial support in *Periconia macrospinosa* isolates and the most significant difference across sites within *Fusarium cf. equiseti* isolates. While isolate results within *F. cf. equiseti* do support our second hypothesis, *Periconia macrospinosa* appear to demonstrate an inverse response. This coupled with the non-significant differences between ED_{50} results across site conditions of the other three species – our second hypothesis was rejected.

To further investigate the underlying mechanisms and differences in adaptive response among conspecific isolates, we designed an experiment in which two isolates, DS 1091 and DS 0982, of *Periconia macrospinosa* that differed most in their salt tolerance as inferred from NaCl ED_{50} estimated in the experiment described above were subjected to prolonged salinity stress followed by proteomic analysis. The selection of *Periconia macrospinosa* isolates over *Fusarium equiseti* isolates was based on the species' critical importance globally in ecosystems experiencing low nutrient and MAP inputs as well as the availability of a recently annotated genome. We hypothesized that (3) the highest and lowest performing strains within a species will differ in their proteomic profiles; (4) colony expansion under saline stress (ED_{50}) will correlate with cell wall related protein abundances under salt stress (signaling cell wall modifications); (5) similarly to the cell wall associated proteins, colony growth (ED_{50}) will correlate with plasma membrane related protein abundances under salt stress (signaling cell membrane alterations); (6) the mitogen-activated protein kinase (MAPK) signaling pathway will be one strategy for

tolerating prolonged salinity amongst the conspecifics (suggesting "compatible-solute" strategy); and, (7) conspecifics associated with the highest ED_{50} will demonstrate greater abundance of proteins involved in salt-tolerant strategies such as cell wall, plasma membrane, and MAPK-related proteins than their counterparts originating from more mesic sites. Our third hypothesis was supported as the two isolates demonstrated unique proteomic profiles both with and without salinity induced responses. Our fourth and fifth hypotheses, which proposed correlation between isolate colony growth and the abundance profiles of proteins involved in cell walls and cell membranes respectively, were also supported by our proteomic data. The fourth hypothesis was reinforced by our proteomic analysis of our high-ED_{50} isolate, DS 0982, through the upregulated chitin synthase coupled with downregulation of chitinase demonstrating an investment in cell wall maintenance. The fifth hypothesis was supported through the evident DS 0982 responses to salinity where indicators of sphingolipid biosynthetic processing and ergosterol biosynthesis were observed. Specifically, support for the cell membrane related protein increase correlated with the colony growth was through ergosterol biosynthesis contributors CDP-diacylglycerol synthase, sterol C-14 reductase-like protein, and sterol 24-C methyltransferase. The sixth hypothesis, which focused on the positive correlation between colony growth and MAPK signaling interactions was also supported. The MAPK high-osmolarity glycerol HOG pathway regulates and initiates osmoadaptive responses within the cell, the most critical of which being the production of the compatible-solute – glycerol. This hypothesis was strongly supported due to observations of abundance differences in response to salinity of several key HOG pathway MAPK proteins, most notably Gdp1 the downstream initiator of glycerol production. Finally, our seventh hypothesis was supported by the observed inverse responses between our two conspecific isolates. As per our hypothesis, the isolate with greatest ED_{50}, DS 0982, did indeed

have the greatest abundance of proteins involved with osmoadaptive strategy across the board from those involved in cell wall modifications such as chitin synthase, to proteins involved in plasma membrane amendments such as including such observations as C-14 reductase-like protein, and even the critical MAPK compatible osmolyte production initiator protein Gdp1.

Understanding soil-inhabiting and root-associated fungi is critical to ecosystem health. Whether through providing nutrient cycling and ecosystem services, or direct interactions with host plants, fungal impacts cannot be ignored. Through the effects of climate change and corresponding changes in precipitation, soil salinization is a major threat to plant and animal health as well as the overall function of our natural world. This research aims to fill the gap in our knowledge on the impact of salinity toward root-associated fungi and their limits in salt-tolerance both within and across species. Further, this study aids in identifying varying functional adaptations soil-dwelling fungi depend on for survival in response to salt stress in soil matrices.

Table of Contents

List of Figures

List of Tables

Acknowledgements

I would like to thank UNM technicians and students Jennifer Bell, Anny Chung, Dylan Kent, and Kendall Beals for assistance with fieldwork and logistics. We thank the students the WIU students Terry Torres-Cruz, Cedric Ndinga Muniania, Terri Tobias, Paris Hamm, Shane Mason, Ryan Deaver, and Maryam Almatruk for their help in the original sample processing, fungal isolation, and sample collection as well as the KSU students Ayanna Castro-Ross, Breanna Jorgensen, and Jenna Wilks for their help in culture maintenance and experimentation using these cultures. We would also like to thank KSU's Vediyappan Lab for their assistance in proteome sample lyophilization and preparation. This work was supported in part by a National Science Foundation (NSF) Division of Environmental Biology (DEB) Award (#1457309), an NSF and Experimental Program to Stimulate Competitive Research (EPSCoR) award (#1656006), and a Department of Energy (DOE) Special Focal Area (SFA) Contract (#385336).

I, Kyle J. Ismert, would also like to take this opportunity to thank all of those who helped me personally in completing this thesis.

First, I would like to thank the SFA team of Pacific Northwest National Laboratory (PNNL) for their countless hours, support, and guidance – in particular: Dr. Janet Jansson, Dr. Christopher Anderton, and Dr. Kirsten Hofmockel. Further, I would especially like to thank Dr. Ernesto Nakayasu and Dr. Geremy Clair for their immeasurable advice, data analytical expertise, assistance with figure development, figure production, writing contributions, and mentorship.

Second, I would like to thank my committee (Dr. Ari Jumpponen, Dr. Lydia Zeglin, Dr. Tom Platt, and Dr. Christopher Little) for their guidance and reassurance throughout my graduate experience with Kansas State University. From coursework and lab experience to professional expertise and personal connection you have all provided me with such an incredible opportunity to learn and grow. To the entire Kansas State University Division of Biology for the irrepressible financial and moral support and infectious camaraderie. Especially Dr. Ari Jumpponen, who provided me with his mentorship, assisted me in performing research, and believed in my abilities. You all have allowed me so much professional and personal growth and I cannot thank you enough.

Finally, I would like to thank my family. To the Millers, thank you for welcoming me into your home and your hearts and for teaching me family is stronger than blood. To the Ismerts, thank you all for teaching me to be strong, persevere, and embrace myself. I would like to acknowledge the contributions by my brother, Jeff Ismert, who assisted in editing and

formatting figures for this research. I would especially like to thank my mother, Jeana, and my father, Matt, who have protected, provided, and sacrificed so much for me to have this blessed life.

To my wife Grace, thank you for inspiring me every day to reach my potential and push myself outside of my comfort zone.

Thank you all for your support, love, and guidance.

Sincerely,

Kyle J. Ismert

Dedication

I would like to dedicate this thesis to my brilliant, resilient, and compassionate wife: Grace M. Ismert. I would not be the man I am today without you.

Thank you,

Kyle J. Ismert

1. Introduction

While it is generally understood that communities of animals, plants, and microorganisms differ along precipitation gradients (Galliart et al. 2020; Eckhart et al. 2004; Anderson et al. 2015; Angel et al. 2010; Williams and Rice 2007; Yom-Tov and Nix 1986; Yom-Tov and Geffen 2006; Pearce-Higgins et al. 2015; Mendola et al. 2015), it remains uncertain whether individuals within species are similarly ecotypically adapted, particularly for microbes. Exacerbated by climate change – increased occurrence and duration of droughts, caused by changes in precipitation, are of particular concern as a threat to water availability in ecosystems (Gautam et al. 2021), especially arid and semi-arid environments where precipitation is low, and evaporation is high (Nachshon 2018). Drier conditions, lesser precipitation, and more frequent drought events all negatively affect available water within a given environment. As water leaves the soil matrix, through evaporation, transpiration, and other means, soluble minerals, namely salts, accumulate and concentrate in soils (Xu et al. 2019). This salinization can have a compounding negative effect on the environment through the effects of decline in plant productivity and vegetation cover (Shrivastava and Kumar 2015). Further, salinization drives changes in activity and composition of microbial communities that lead to decreased nutrient cycling and ecosystem services (Rath and Rousk 2015; Yan et al. 2015). This compounds into further issues through decreased organic inputs – aiding in desertification (Sentis 1996; Hassani et al. 2020). Soil-inhabiting microbes in particular often encounter the negative effects of saline conditions (Yan et al. 2015). Among soil-inhabiting microbes, root-associated fungi are especially powerful regulators of plant success. These fungi act as mutualistic symbionts, latent pathogens, and/or saprotrophs (Porras-Alfaro and Bayman 2011; Fesel and Zuccaro 2016), while providing a range

of other ecosystem services ranging from nutrient and water allocation and nutrient cycling to even functions as bioprotectors and deterrents of plant disease (Xavier and Boyetchko 2003).

Coupled with their numerous interactions with plants, especially their critical role in salt stress-mediation (Li et al. 2017), it is imperative to understand how saline stress might affect microbes associated with plants, especially fungi. Fungi are more tolerant to salt stress than bacteria (Rath et al. 2016) and have also been reported to improve plant host salt-stress tolerance (Dastogeer et al. 2020; Evelin et al. 2019; Begum et al. 2019; Li et al. 2017). Soil salinization, *i.e*., the increase and accumulation of salts in soil water, is a gradually increasing concern because of its potential implications on plant and microbial health. There is also evidence of accelerated soil salinization due to direct and indirect effects of climate change correlate with increases in temperature and decreases in precipitation (Okur and Örçen 2020). To better understand the ecotypic adaptive response of root-associated fungi to salinity, we designed an experiment to test the salt tolerance of thirty fungal isolates representing five ascomycete species or species complexes from sites that experience two-fold differences in mean annual precipitation (MAP) across the central United States.

In the soil system, salts concentrate as water availability declines within the soil substrate. The increasing salt ion concentration results in salt-stress for fungi within the soil matrix through actions of osmotic stress, intracellular water loss, and ion toxicity. However, fungi can combat salt-stress disequilibrium through one of two primary strategies: 1) “salt-in” and 2) “compatible-solute” otherwise known as “salt-out” (Gunde-Cimerman et al. 2018). The “salt-in” strategy is rather rare and involves taking salts from the environment into the cell and tolerating or compartmentally storing excess salts in order to maintain aqueous equilibrium. However, this concentration of salts within the cell can be very damaging and potentially fatal to

the cell and the whole organism. As a result, fungi primarily use the “compatible-solute” or “salt-out" strategy through specialized responses to salt stress via actions of cell wall modification (Hagiwara et al. 2015), changes in membrane composition (Gostinčar et al. 2011; Pascual-Ahuir et al. 2018), and cytosolic osmolyte accumulation (Klein et al. 2016; Konte et al. 2016). It is likely, however, that cells may use some combination of the two strategies to tolerate high salinity. Fungi activate “compatible solute” strategy processes through several functional systems – most notably, a highly conserved signaling pathway, the MAPK signaling pathway, has often been reported in fungi as a response regulator to osmotic stress and ion homeostasis (Hohmann 2002), predominantly through the production of the compatible solute, glycerol (Kayingo and Wong 2005). While the majority of studies have focused on halotolerant and xerotolerant extremophiles (Lebre et al. 2017; Buzzini et al. 2018), model fungi (Stratford et al. 2019), or human pathogens or microbiome associates (Jacobson et al. 2018) – similar studies on soil-inhabiting or root-associated fungi are rare.

To investigate salinity tolerances of soil and root-inhabiting fungi and their avoidance of the detrimental effects of salinity, we chose conspecific isolates or species complexes of five ascomycetes across a precipitation gradient. Using proteomic analyses, we aimed to identify the mechanisms that underlay the adaptive tolerances of select isolates that differed in their experimentally determined salt-tolerances. Based on the observed ED_{50} results, we chose a salinity of 25g/L (0.4 M) to investigate salinity responses in a prolonged challenge, this coincided with the commonly used 0.4 M salinity challenge published in established research (Babazedah et al. 2017; Stojanovski et al. 2017; Tatebayashi et al. 2020). Most studies that focus on saline stress choose a brief saline shock (e.g., Brewster et al. 1993; Schüller et al. 1994; Szopinska et al. 2011; Babazedah et al. 2017; Tatebayashi et al. 2020). However, these designs

poorly account for prolonged or continuous salt challenges more akin to conditions experienced by soil-inhabiting organisms during periods of low water availability and concurrent salinity stress. In an effort to uncover the responses to prolonged salt-mediated osmostress, we combined proteomic analyses with selection of conspecific isolates selected for their differing tolerances to salt.

While it is generally understood that species of fungi and ascomycetes in general differ in their responses to salt (Motoyama et al. 2005), it is less well understood if salt responses differ among conspecific strains within species. To investigate the inter- and intraspecific adaptive responses of root-associated ascomycetes to saline stress, we devised an experiment where five species or species complexes of ascomycetes, each with three conspecifics originating from drier "arid" environments and three conspecifics originating from wetter "mesic" environments, were subjected to increasing concentrations of salt (NaCl) in an effort to quantify and compare their salt tolerances. We estimated the effective NaCl dose necessary to limit colony growth of our isolates by 50% (ED_{50}). We hypothesized that (1) ascomycetes differ in their growth response to salinity across species; (2) conspecific strains from drier sites have greater salt tolerance than those from more mesic sites. To further investigate the underlying mechanisms and differences in adaptive responses within species, we designed an experiment in which two conspecifics, which differed most in their estimated ED_{50} and originated from different environments which varied in precipitation were subjected to prolonged salinity stress. We chose the ecologically important root-associated ascomycete, *Periconia macrospinosa*, and analyzed two conspecific isolates for differences in their proteomic responses to salt stress. We hypothesized that (3) conspecifics differing most in ED_{50} will also differ in their proteomic profiles; (4) responses in colony growth to salt stress (ED_{50}) will correlate with cell wall related protein abundances under

salt stress (indicating cell wall modifications); (5) responses in colony growth to salt stress (ED_{50}) will correlate with plasma membrane related protein abundances under salt stress (indicating cell membrane alterations); (6) the MAPK signaling pathway will be among the strategies for tolerating prolonged salinity amongst conspecifics (suggesting "compatible-solute" strategy); and, (7) conspecifics with higher ED_{50} will demonstrate greater abundance of proteins involved in salt-tolerant strategies such as cell wall, plasma membrane, and MAPK-related proteins than their counterparts with lower ED_{50}.

Understanding how soil-inhabiting and root-associated fungi respond to salinity and maintain their metabolic activities is critical to ecosystem health. Whether through providing nutrient cycling and ecosystem services, or direct interactions with host plants, importance of fungi and their functions under environmental stress cannot be overstated. Through the effects of climate change and lower precipitation, soil salinization is a major threat to plant and animal health as well as to the overall ecosystem function. This research aims to fill a gap in our knowledge on the impact of salinity on the root-associated fungi and their limits in salt-tolerance both within and across species. Further, this study aids in identifying the varying functional adaptations soil-dwelling fungi depend on for survival in response to salt stress in soil matrices.

References

Anderson JT, Eckhart VM, Geber MA. 2015. Experimental studies of adaptation in *Clarkia xantiana*. III. Phenotypic selection across a subspecies border. Evolution. 69(9):2249–2261.

Angel R, Soares MI, Ungar ED, Gillor O. 2010. Biogeography of soil archaea and bacteria along a steep precipitation gradient. ISME J. 4(4):553-563.

Babazadeh R, Lahtvee PJ, Adiels CB, Goksör M, Nielsen JB, Hohmann S. 2017. The yeast osmostress response is carbon source dependent. Sci Rep. 7(1):990.

Begum N, Qin C, Ahanger MA, Raza S, Khan MI, Ashraf M, Ahmed N, Zhang L. 2019. Role of Arbuscular Mycorrhizal Fungi in Plant Growth Regulation: Implications in Abiotic Stress Tolerance. Front Plant Sci. 10:1068.

Dastogeer KMG, Zahan MI, Tahjib-Ul-Arif M, Akter MA, Okazaki S. 2020. Plant Salinity Tolerance Conferred by Arbuscular Mycorrhizal Fungi and Associated Mechanisms: A Meta-Analysis. Frontiers in Plant Science. 11:1927.

Eckhart VM, Geber MA, McGuire CM. 2004. Experimental studies of adaptation in *Clarkia xantiana*. I. Sources of trait variation across a subspecies border. Evolution. 58(1):59– 70.

Evelin H, Devi TS, Gupta S, Kapoor R. 2019. Mitigation of Salinity Stress in Plants by Arbuscular Mycorrhizal Symbiosis: Current Understanding and New Challenges. Frontiers in Plant Science. 10:470.

Fesel PH and Zuccaro A. 2016. Dissecting endophytic lifestyle along the parasitism/mutualism continuum in Arabidopsis. Curr. Opin. Microbiol. 32:103–112.

Galliart M, Sabates S, Tetreault H, DeLaCruz A, Bryant J, Alsdurf J, Knapp M, Bello NM, Baer SG, Maricle BR, Gibson DJ, Poland J, Amand PS, Unruh N, Parrish O, Johnson LC. 2020. Adaptive genetic potential and plasticity of trait variation in the foundation prairie grass Andropogon gerardii across the US Great Plains' climate gradient: Implications for climate change and restoration. Evolutionary Applications. 13(9):2333-2356.

Gautam S, Costello C, Baffaut C, Thompson A, Sadler EJ. 2021. Projection of future drought and extreme events occurrence in Goodwater Creek Experimental Watershed, Midwestern US. Hydrological Sciences Journal. 66(6):1045-1058.

Gostinčar C, Lenassi M, Gunde-Cimerman N, Plemenitaš A. 2011. Fungal Adaptation to Extremely High Salt Concentrations. Advances in Applied Microbiology. 3(77):71-96.

Gunde-Cimerman N, Plemenitaš A, Oren A. 2018. Strategies of adaptation of microorganisms of the three domains of life to high salt concentrations. FEMS Microbiology Reviews. 42(3):353–375.

Hagiwara D, Yoshimi A, Sakamoto K, Gomi K, Abe K. 2015. Response and adaptation to cell wall stress and osmotic stress in *Aspergillus* species. Stress Biology of Yeasts and Fungi. Tokyo: Springer Japan. 2015:199–218.

Kayingo G and Wong B. 2005. The MAP kinase Hog1p differentially regulates stress-induced production and accumulation of glycerol and D-arabitol in *Candida albicans*. Microbiology. 151(9):2987-2999.

Klein M, Swinnen S, Thevelein JM, Nevoigt E. 2016. Glycerol metabolism and transport in yeast and fungi: established knowledge and ambiguities. Environmental Microbiology. 19(3):878-893.

Konte T, Terpitz U, Plemenitaš A. 2016. Reconstruction of the High-Osmolarity Glycerol (HOG) Signaling Pathway from the Halophilic Fungus *Wallemia ichthyophaga* in Saccharomyces cerevisiae. Front. Microbiol. 7:901.

Li X, Han S, Wang G, Liu X, Amombo E, Xie Y, Fu J. 2017. The Fungus Aspergillus aculeatus Enhances Salt-Stress Tolerance, Metabolite Accumulation, and Improves Forage Quality in Perennial Ryegrass. Front Microbiol. 8:1664.

Mendola ML, Baer SG, Johnson LC, Maricle BR. 2015. The role of ecotypic variation and the environment on biomass and nitrogen in a dominant prairie grass. Ecology. 96(9):2433–2445.

Motoyama T, Kadokura K, Ohira T, Ichiishi A, Fujimura M, Yamaguchi I, Kudo T. 2005. A two-component histidine kinase of the rice blast fungus is involved in osmotic stress response and fungicide action. Fungal Genetics and Biology. 42(3):200-212.

Okur B and Örçen N. 2020. Chapter 12 - Soil salinization and climate change. In: Prasad MNV and Pietrzykowski M, eds. Climate Change and Soil Interactions. Elsevier. 2020:331-350.

Paix MJ, Lanhai L, Xi C, Varenyam A, Nyongesah MJ, Habiyaremye G. 2011. Physicochemical properties of saline soils and aeolian dust. Land Degradation and Development. 24:539–547.

Pascual-Ahuir A, Manzanares-Estreder S, Timón-Gómez A, Proft M. 2018. Ask yeast how to burn your fats: lessons learned from the metabolic adaptation to salt stress. Curr Genet. 64:63–69.

Pearce-Higgins JW, Ockendon N, Baker DJ, Carr J, White EC, Almond REA, Amano T, Bertram E, Bradbury RB, Bradley C, Butchart SHM, Doswald N, Foden W, Gill DJC, Green RE, Sutherland WJ, and Tanner EVJ. 2015. Geographical variation in species' population responses to changes in temperature and precipitation. Proc Biol Sci. 282(1818):20151561.

Porras-Alfaro A and Bayman P. 2011. Hidden Fungi, Emergent Properties: Endophytes and Microbiomes. Annu. Rev. Phytopathol. 49:291–315.

Rath KM and Rousk J. 2015. Salt effects on the soil microbial decomposer community and their role in organic carbon cycling: A review. Soil Biol. Biochem. 81:108–123.

Rath KM, Maheshwari A, Bengtson P, Rousk J. 2016. Comparative Toxicities of Salts on Microbial Processes in Soil. Appl Environ Microbiol. 82(7):2012-2020.

Sentis IP. 1996. Soil salinization and land desertification" in Soil Degradation and Desertification in Mediterranean Environments. Geoforma Ediciones. 1996:105–129.

Shrivastava P and Kumar R. 2015. Soil salinity: A serious environmental issue and plant growth promoting bacteria as one of the tools for its alleviation. Saudi J Biol Sci. 22(2):123-131.

Stojanovski K, Ferrar T, Benisty H, Uschner F, Delgado J, Jimenez J, Solé C, Nadal E, Klipp E, Posas F, Serrano L, Kiel C. 2017. Interaction Dynamics Determine Signaling and Output Pathway Responses. Cell Rep. 19(1):136-149.

Tatebayashi K, Yamamoto K, Tomida T, Nishimura A, Takayama T, Oyama M, Kozuka-Hata H, Adachi-Akahane S, Tokunaga Y, Saito H. 2020. Osmostress enhances activating phosphorylation of Hog1 MAP kinase by mono-phosphorylated Pbs2 MAP2K. EMBO Journal. 39:e103444.

Williams MA and Rice CW. 2007. Seven years of enhanced water availability influences the physiological, structural, and functional attributes of a soil microbial community. Appl. Soil Ecol. 35:535–545.

Xavier LJC and Boyetchko SM. 2003. Arbuscular Mycorrhizal Fungi in Plant Disease Control. https://doi.org/10.1201/9780203913369.ch16

Xu J, Lan W, Li Y, Cheng W, Yuan J, Tan Q. 2019. Evaporation-Induced Water and Solute Coupled Transport in Saline Loess Columns in Closed and Open Systems. Hindawi Geofluids. 2019:3781410.

Yan N, Marschner P, Cao W, Zuo C, Qin W. 2015. Influence of salinity and water content on soil microorganisms. International Soil and Water Conservation Research. 3(4):316-323.

Yom-Tov Y and Geffen E. 2006. Geographic Variation in Body Size: The Effects of Ambient Temperature and Precipitation. Oecologia, 148(2):213–218.

Yom-Tov Y and Nix H. 1986. Climatological Correlates for Body Size of 5 species of Australian Mammals. Biological journal of the Linnean Society. 29(4):245-262.

2. Methods

Sample Collection

In the course of a larger environmental survey of fungi to evaluate the impact of drought, geography, and plant traits or edaphic and environmental factors on fungal communities across latitudinal and longitudinal gradients in North America (Jumpponen et al. 2017; Lagueux et al. 2020; Rudgers et al. 2022), we established a collection of 1,033 pure cultures isolated in the summer of 2016. In that study, roots from foundation grass species – blue grama (*Bouteloua gracilis* (Willd. ex Kunth) Lag. ex Griffiths), black grama (*B. eriopoda* (Torr.) Torr.), side oats grama (*B. curtipendula* (Michx.) Torr.), big bluestem (*Andropogon gerardii* Vitman), and little bluestem (*Schizachyrium scoparium* (Michx.) Nash) – were collected from 23 sites in south central states in the United States. At each site, a total of twelve whole plants were excavated with a transplanting shovel as described in Mandyam et al. (2012), and root systems were sampled for pure culturing at Western Illinois University (WIU; Macomb, IL) within 48 hours of collection.

Fungal Isolation and Identification

Methods for fungal isolation and identification have been described previously in Rudgers et al. (2022). Briefly, following sample collection and removal of adhering soil and debris, foundation grass roots were cut into 1 cm long segments then surface sterilized with 70% ethanol for 1 minute, with 1% bleach for 1 minute, rinsed three times with sterilized distilled water, and aseptically cut again into three smaller segments each ~3 mm in length. Six of these smaller root segments from each sample were randomly selected and plated on malt extract agar (MEA) (Difco Laboratories, Detroit, MI, USA) amended with antibiotics to prevent bacterial growth (Streptomycin and Tetracycline, 50 mg/L) on 48-well plates (Fisher Scientific, Walham, MA). The surface sterilization was confirmed by pressing sterilized roots on MEA – these

controls did not yield growth. The MEA plates were wrapped in parafilm and incubated at room temperature (25°C) for two weeks. After two weeks, different morphologies were transferred onto small Petri dishes (50 mm) of MEA amended with antibiotics (Streptomycin and Tetracycline, 50 mg/L). Representatives of the cultures are maintained at the WIU Fungarium and at the University of New Mexico (UNM; Albuquerque, NM) in cryovials with 1000 µL sterile water (Rudgers et al. 2022).

For molecular identification, the genomic DNA was extracted from the cultured isolates using Wizard genomic DNA purification kits (Promega, Madison, Wisconsin) following the manufacturer's protocol. Fungal barcode marker (Schoch et al. 2012) – the Internal Transcribed Spacer (ITS) of the ribosomal RNA gene repeat – was PCR-amplified using primers ITS1F (Gardes and Bruns 1993) and ITS4 (White et al. 1990). The 25µl PCR reactions contained 12.5 µl of GoTaq PCR master mix (Promega, Madison, Wisconsin), 3 µl of 1% bovine serum albumin (BSA), 1 µl of each primer (5µM), 6.5 µl of nuclease-free water and 1 µl of genomic DNA. PCR reactions included an initial denaturation at 95 °C for 5 min; 35 cycles of denaturation at 94 °C for 30s, annealing at 50 °C for 30s, and extension at 72 °C for 45s; and a final extension at 72 °C for 7 min. Molecular grade water was used as negative controls.

The PCR amplicons were visualized by gel electrophoresis on 1.2% TAE (Tris-acetate-EDTA agarose). The PCR amplicons were sequenced with the forward primer (ITS1F) at Beckman Coulter Genomics (Danvers, Massachusetts). Obtained sequences were trimmed and edited using Sequencher 4.1 (Gene Codes, Ann Arbor, Michigan). Fungal isolates were assigned to taxa using the Basic Local Alignment Search Tool (BLAST) (Altschul et al. 1997) and UNITE (Kõljalg et al. 2013). The ITS sequence data are available at the National Center for Biotechnology Information (NCBI) GenBank (accession numbers are listed in Table 1).

Strain Selection

For the current study, we exploited this culture collection and sampling scheme to select, based on 99% ITS sequence similarity, groups of putatively conspecific ascomycete isolates for a balanced experimental design such that half of the isolates originated from either arid or mesic sites. We defined arid sites as those with a Mean Annual Precipitation (MAP) less than 600 mm, whereas mesic sites were those with a MAP greater than 600 mm. We selected a total of five species or species complexes, each with three strains from arid and three strains from mesic sites for a total of thirty strains. These isolates originated from a total of eight sites and from four different plant species (Table 1). A complete list of isolate species, strain, host, and site information is listed in the supplemental material (Table S1). The selection of thirty strains was shipped on MEA petri plates on ice to Kansas State University where they were transferred to Petri plates with potato dextrose agar (PDA) (Difco Laboratories, Detroit, MI, USA).

Species	Isolate ID	GenBank Accession Number	Host	Site	Arid/Mesic
Curvularia spicifera	DS 1212	MK808194	BOGR	SEV	Mesic
Curvularia spicifera	DS 1303	MK808270	BOGR	SEV	Mesic
Curvularia spicifera	DS 1304	MK808271	BOGR	SEV	Mesic
Curvularia spicifera	DS 0901	MK808983	BOGR	KNZ	Arid
Curvularia spicifera	DS 0902	MK808984	BOGR	KNZ	Arid
Curvularia spicifera	DS 1246	MK808225	BOGR	KNZ	Arid
Fusarium equiseti complex	DS 0607	MK808833	BOER	NWP	Mesic
Fusarium equiseti complex	DS 0608	MK808834	BOER	NWP	Mesic
Fusarium equiseti complex	DS 0614	MK808841	BOER	NWP	Mesic
Fusarium equiseti complex	DS 1641	MK808498	BOER	CNF	Arid
Fusarium equiseti complex	DS 1645	MK808501	BOER	CNF	Arid

Fusarium equiseti complex	DS 1651	MK808506	BOER	CNF	Arid
Fusarium chlamydosporum complex	DS 0682	MK808867	BOGR	KNZ	Mesic
Fusarium chlamydosporum complex	DS 0687	MK808869	BOGR	KNZ	Mesic
Fusarium chlamydosporum complex	DS 0695	MK808872	BOGR	KNZ	Mesic
Fusarium chlamydosporum complex	DS 1435	MK808365	BOGR	HPG	Arid
Fusarium chlamydosporum complex	DS 1437	MK808367	BOGR	HPG	Arid
Fusarium chlamydosporum complex	DS 1438	MK808368	BOGR	HPG	Arid
Periconia macrospinosa	DS 0981	MK809059	BOCU	KNZ	Mesic
Periconia macrospinosa	DS 0982*	MK809060	BOCU	KNZ	Mesic
Periconia macrospinosa	DS 0984	MK809062	BOCU	KNZ	Mesic
Periconia macrospinosa	DS 1091*	MK808096	BOCU	HAR	Arid
Periconia macrospinosa	DS 1094	MK808099	BOCU	HAR	Arid
Periconia macrospinosa	DS 1095	MK808100	BOCU	HAR	Arid
Trichoderma gamsii	DS 0430	MK808752	BOER	BNP	Mesic
Trichoderma gamsii	DS 0432	MK808754	BOER	BNP	Mesic
Trichoderma gamsii	DS 0444	MK808766	BOER	BNP	Mesic
Trichoderma gamsii	DS 0071	MK808879	SCSC	LBJ	Arid
Trichoderma gamsii	DS 0073	MK808885	SCSC	LBJ	Arid
Trichoderma gamsii	DS 0075	MK808891	SCSC	LBJ	Arid

Table 1. The ascomycete isolates used in the ED_{50} studies. Isolate ID refers to accession numbers in the WIU Fungarium; GenBank Accession refers to ITS sequence data deposited to NCBI GenBank; hosts are *Bouteloua gracilis* (BOGR), *Bouteloua eriopoda* (BOER), *Bouteloua curtipendula* (BOCU), *Schizachyrium scoparium* (SCSC); sites are Sevilleta National Wildlife Refuge (SEV) [242 mm MAP], Konza Prairie Biological Station (KNZ) [860 mm MAP], Nickel Family Nature and Wildlife Preserve (NWP) [1,276 mm MAP], Carson National Forest (CNF) [321 mm MAP], High Plains Grassland Research Center (HPG) [384 mm MAP], Hays Agricultural Research Center (HAR) [577 mm MAP], Big Bend National Park (BNP) [384 mm MAP], Ladybird Johnson Wildflower Center (LBJ) [870 mm MAP]; and, Arid sites have MAP <600 mm/year, whereas Mesic sites have MAP >600 mm/year. Asterisks (*) identify isolates selected for the proteomic analysis.

NaCl Tolerance ED_{50} Estimation through Regression Analysis

To expediently assess NaCl-tolerance of the selected fungal cultures, we used quad dishes (Thermo Fisher Scientific, Inc., Waltham, MA, USA; Cat. No. FB087582) with their four quadrants filled with 10ml PDA amended with either 0g/l, 25g/l, 50g/l, or 100g/l NaCl. This way, each plate represented a full replicate of complete NaCl concentration gradient that we used to estimate NaCl concentration that reduced the colony expansion by 50% (Effective Dose or ED_{50}). The fungal cultures were transferred onto the quad dishes from standard Petri plates (100 mm × 15 mm) with 20ml PDA. We selected large, two-centimeter (diameter) inoculum plugs to enable pressing the inoculum such that it reached each of the four sectors of the quad dish. The inoculum plugs were excised with a cork borer from one-week old cultures and pressed firmly, hyphal side down, to the center of each quad dish. Growth – the increase in the colony radius – within each quadrant was recorded daily until any one isolate of a species reached the plate's edge in the quadrant without any additional NaCl. Terminal data point was recorded at this time for all isolates of that species and recording was not continued further.

Species differed in their growth rates (Fig. 1). As a result, the incubation times varied from five to seven days among the species but were identical for all the conspecific strains. A complete list of growth rates and incubation times is located in the supplemental material (Table S2). The different incubation times permitted recording colony expansion adequately for taxa that varied in their growth rates. The NaCl challenges were repeated three times for each isolate in a non-replicated temporal block design, in which all thirty fungal strains were grown in a temporal block and each block was replicated three times.

The colony growth data were used to estimate the effective dose that reduced the colony growth by 50% (ED_{50}) (Dixon and Mood 1948; OECD 2000a; OECD 2000b) to compare NaCl

tolerances among the thirty selected isolates. We estimated ED_{50} individually for each of the six replicates of the thirty isolates – in our experimental design each quad dish represented one independent experimental unit yielding one ED_{50} estimate, allowing for a total of six replicate ED_{50} estimates for each isolate. To estimate ED_{50}, we regressed the final colony radius (measured from the edge of colony to the edge of the inoculum plug) within each quadrant against the NaCl concentration and estimated the concentration that reduced the colony growth by 50% from that in the non-amended quadrant.

NaCl Tolerance Statistical Analyses

Statistical analyses were executed using JMP® software version 15.0 (SAS Institute Inc., Cary, North Carolina). Differences in the ED_{50} estimates ($\alpha = 0.05$) were tested to compare i) overall NaCl tolerance across all isolates originating from either arid or mesic sites in a mixed effect analysis of variance (ANOVA) with "species" assigned as a random effect and "climate" MAP at the origin of the strain (arid vs. mesic) as a fixed effect; ii) species and their NaCl tolerances depending on MAP at the site of isolate origin in a mixed effect ANOVA with "block" assigned as a random effect to account for the strains as replicate without exaggerating the statistical power in our analyses and the main effects "species" and "climate" as well as their interaction as fixed effects; and, iii) NaCl tolerance of strains within each species originating either from arid or mesic sites in one-way ANOVA as shown in Fig. 1. We selected *Periconia macrospinosa* as a focal species for proteome analyses (below). For the selected two strains with the most extreme ED_{50} estimates, we further tested for differences in their growth in a mixed effect ANOVA with "block" as a random effect and "strain" and NaCl concentration "[NaCl]" as the fixed effects (see Fig. 2).

Sample Preparation for the Proteomics Analyses

Based on the recorded ED_{50} estimates and our literature review, we chose a mild salinity of ~0.4M NaCl (Brewster et al. 1993; Schüller et al. 1994; Szopinska et al. 2011; Babazedah et al. 2014; Stojanovski et al. 2017; Babazedah et al. 2017; Tatebayashi et al. 2020) to investigate responses in a prolonged NaCl challenge. While most studies choose brief saline shock (e.g., Babazedah et al. 2017; Stojanovski et al. 2017; Tatebayashi et al. 2020), these designs do not account for the effects of prolonged or continual salt challenges more akin to the conditions experienced by organisms in their natural environments during periods of low water availability. From the five species observed in the ED_{50} analyses, we chose *P. macrospinosa* for further proteomic investigation based on its growth response to NaCl, hypothesized function in host salt tolerance as well as its ubiquitous, global presence in grassland systems (Mandyam and Jumpponen 2005), previous examples of reliable ITS barcode-based taxon identification (O'Donnell 2010), proposed important ecological role in arid and nutrient-limited ecosystems and availability of a recently available annotated genome (Knapp et al. 2018). To better understand the effects of prolonged salt stress, we grew the two *P. macrospinosa* isolates with the most extreme (high and low) ED_{50} estimates for two weeks (14 days) in preparation for advanced proteomic analysis. Chosen isolates (DS 0982 and DS 1091; Table 1) were grown in quadruplicate on 20ml of solid media in parafilm sealed Petri dishes under two NaCl conditions: i) control (PDA with no amended NaCl [0M NaCl]) and ii) experimental (PDA amended with 25g/L NaCl [0.43M NaCl]). Two weeks post-inoculation, the total 16 proteomic samples (2 strains x 2 NaCl concentrations x 4 replicates) were subsequently transferred into 50ml Falcon tubes, parafilm sealed, and stored at -80° C.

Less than 48 hours following cold storage, the samples were prepared for lyophilization. The tissues were lyophilized at -50° C under a high vacuum for 16 hours. Following lyophilization the dried samples were stored at -20 C° for less than 24 hours prior to shipping to Pacific Northwest National Laboratory's (PNNL) Environmental Molecular Sciences Laboratory (EMSL) on dry ice for further protein extraction and proteome analysis. The hyphal biomass was extracted in microcentrifuge tubes with beads (Omni International, Kennesaw, GA) and 50 mM $NH4HCO_3$ (pH 8), and lysed using a bead ruptor elite (Omni International, Kennesaw, GA) tissue lyser by homogenizing twice at 6 rpm for 45 s. The microcentrifuge tube with the cell lysate was placed over a 15 ml falcon tube after a hole was poked in the microcentrifuge tube using a 26-gauge needle and the lysate extracted by centrifuging at 4500 x g for 5 min. The microcentrifuge tube with beads was washed using ammonium bicarbonate solution and centrifuged again at 4500 x g for 5 min. The lysates from the two wash cycles were combined.

A solution of 2:1 chloromethane:methanol (CH_3Cl:CH_3OH) was added at 5 times the volume of the cell lysate and vortexed for 30 s and kept on ice for 5 min and vortexed again for 30 s. The solution was centrifuged at 10000 x g for 10 min at 4˚C and the protein interlayer was collected and dissolved in 8 M urea. A bicinchoninic acid (BCA) protein assay (Smith et al. 1985) was performed to determine the amount of protein in each sample before further analysis using the global digestion protocol. The protein interlayer solution in urea was then incubated at 60˚C after adding dithiothreitol (Sigma Aldrich, St. Louis, MO) at 5 mM concentration for 30 min. The sample was diluted 10-fold in 50 mM NH_4HCO_3 and $CaCl_2$ was added to a concentration of 1 mM. Protein digestion was performed by incubating in trypsin (1 µg trypsin/50 µg protein: Thermo Fisher Scientific, Waltham, MA) for 3 h. The samples were

desalted using 30 mg/ml C18 polymeric reversed phase column (Strata-X 33u, Phenomenex, Torrance, CA) and analyzed using liquid chromatography mass spectrometry (LCMS).

Liquid Chromatography Mass Spectrometry (LCMS) of Protein Digests

A nanoACQUITY ultra performance liquid chromatography (LC) with a 2DLC system (Waters, Milford, MA, USA) was used to separate protein digests. Buffer A (0.1% formic acid in water) and buffer B (0.1% formic acid in acetonitrile) were used as mobile phases for a 180 min gradient separation. A 5 µl protein digests were automatically loaded onto a C18 reversed phase column prepared in-house (70 cm x 70 µm I.D. with 3 µm Jupiter C18 particle size, room temperature) with 100% buffer A at 5 µl/min. The eluted peptides from the C18 column were analyzed using a Q-Exactive Plus Orbitrap MS (Thermo Scientific, San Jose, CA) for high resolution MS and high-energy collision-induced dissociation tandem MS by electrospray ionization. Samples were analyzed using a 180 min LC-MS/MS method, data acquisition was started 15 min after sample injection. Spectra were collected between 375 to 1800 m/z at a mass resolution of 180000 (at m/z 200), followed by a maximum ion trap time of 180 ms. Peptides were fragmented using a high-energy collision energy level of 32% and a dynamic exclusion time of 30 s for discriminating against previously analyzed ions.

Quantitative Analysis and Data Integration

Proteins were compared based on relative abundances and were considered up- or down-regulated at alpha with a *P*-value of ≤ 0.05 in comparative *t*-tests. Missing values, for *t-test* comparison analysis, were overwritten with half of the smallest value within the data set. Using the Multi-Experiment Viewer (MeV, v4.9.0) (Howe et al. 2011), orthologues were grouped into

five clusters, clusters generated using k-means, and integrated into a heatmap (Figure 3). Using key-word searches, proteins assigned to the cell wall and cell membrane related processes were compared in heatmaps generated in MeV and represented in Figures 4 and 5, respectively. A complete list of cell wall proteins utilized for analysis and generation of Figure 4 (Table S6) and a complete list of cell membrane proteins used for creating Figure 5 (Table S7) are listed in the supplementary materials.

Proteins were annotated using the KEGG (Kyoto Encyclopedia of Genes and Genomes) database (Kanehisa and Goto 2000; Kanehisa 2019; Kanehisa et al. 2021) to map KEGG Orthology (KO) terms to protein orthologues through the assignment of a K number. The K number assignment was performed via KEGG's internal annotation implement, KOALA (KEGG Orthology And Links Annotation) (Kanehisa et al. 2016a) coupled with a rapid GhostX sequence data search through the use of the GhostKOALA program (Kanehisa et al. 2016b). Following the KEGG annotation, a KEGG pathway enrichment analysis was performed for each of the five clusters using Microsoft Access Database to map KEGG annotations to relative and standardized (via Fisher exact test cut-off) quantitative protein abundances and Microsoft Excel (Microsoft Office 2019, v16.50) to perform enrichment analysis. Enrichment analysis utilized Fisher exact tests and only enrichment *P*-values of ≤ 0.05 were considered significant.

KEGG pathway enrichment highlighted a key MAPK Signaling Pathway considered to be critical in cell signaling, regulation, and osmotic response. KEGG's GhostKOALA annotation of this pathway of interest was referenced to the more comprehensive annotations of the model fungus *Saccharomyces cerevisiae*. The MAPK signaling pathway is composed of several highly conserved components thought to be crucial across Kingdom Fungi. Thus, *S. cerevisiae* has been deemed an ideal MAPK model system in functional analyses of orthologous proteins involved in

fungal signaling (Bansal et al. 2001; El-Mowafy et al. 2013; Konte et al. 2016). Consistent with this, *S. cerevisiae* MAPK signaling proteins in our findings present consistent homologues across fungi regardless of evolutionary relationship, categorization, or survival strategy (Martínez-Soto and Ruiz-Herrera 2017).

To further investigate this pathway, and in particular its role in regulating osmotic response affected by salinity, we used an integrated data pathway visualization software, the Visualization and Analysis of Networks con-Taining Experimental Data tool (VANTED, v2.8.1) (Junker et al. 2006; Rohn et al. 2012). The VANTED software is a powerful tool for -omics related studies and allows for the analyses of large, complex datasets in order to provide insight on expressed and detected pathway responses and biological functions (Hartmann and Jozefowicz 2018). A subsection of the MAPK Signaling Pathway known as the High-Osmolarity Glycerol (HOG) pathway was manually developed by integrating protein data into a VANTED pathway (Figure 5). The HOG pathway proteins were considered differentially regulated at (α= 0.05) in *t-tests*.

References

Altschul SF, Madden T, Schäffer AA, Zhang J, Zhang Z, Miller W, Lipman DJ. 1997. Gapped BLAST and PSI-BLAST: a new generation of protein database search programs. Nucleic Acids Research 25:3389-3402.

Babazadeh R, Lahtvee PJ, Adiels CB, Goksör M, Nielsen JB, Hohmann S. 2017. The yeast osmostress response is carbon source dependent. Sci Rep. 7(1):990.

Brewster JL, de Valoir T, Dwyer ND, Winter E, Gustin MC. 1993. An osmosensing signal transduction pathway in yeast. Science. 259(5102):1760-1763.

Dixon WJ and Mood AM. 1948. A Method for Obtaining and Analyzing Sensitivity Data. Journal of American Statistics Association. 43:109-126.

Gardes M and Bruns J. 1993. ITS primers with enhanced specificity for basidiomycetes application to the identification of mycorrhizae and rusts. Molecular Ecology. 2:113-118.

Hartmann A and Jozefowicz AM. 2018. VANTED: A Tool for Integrative Visualization and Analysis of -Omics Data. Methods Mol Biol. 1696:261-278.

Howe EA, Sinha R, Schlauch D, Quackenbush J. 2011. RNA-Seq analysis in MeV. Bioinformatics. 27:3209-3210.

Jumpponen A, Herrera J, Porras-Alfaro A, Rudgers J. 2017. Biogeography of root-associated fungal endophytes. Ecological Studies. 230:195-222.

Junker BH, Klukas C, Schreiber F 2006. VANTED: a system for advanced data analysis and visualization in the context of biological networks. BMC Bioinformatics. 7(109):1-13

Kanehisa M and Goto S. 2000. KEGG: Kyoto Encyclopedia of Genes and Genomes. Nucleic Acids Res. 28:27-30.

Kanehisa M, Furumichi M, Sato Y, Ishiguro-Watanabe M, Tanabe M. 2021. KEGG: integrating viruses and cellular organisms. Nucleic Acids Res. 49:545-551.

Kanehisa M, Sato Y, Kawashima K, Furumichi M, Tanabe M. 2016a. KEGG as a reference resource for gene and protein annotation. Nucleic Acids Res. 44:457-462.

Kanehisa M, Sato Y, Morishima K. 2016b. BlastKOALA and GhostKOALA: KEGG tools for functional characterization of genome and metagenome sequences. J. Mol. Biol. 428:726-731.

Kanehisa M. 2019. Toward understanding the origin and evolution of cellular organisms. Protein Sci. 28:1947-1951.

Kõljalg U, Nilsson RH, Abarenkov K, Tedersoo L, Taylor AF, Bahram M, Bates ST, Bruns TD, Bengtsson-Palme J, Callaghan TM, Douglas B, Drenkhan T, Eberhardt U, Dueñas M,

Grebenc T, Griffith GW, Hartmann M, Kirk PM, Kohout P, Larsson E, Lindahl BD, Lücking R, Martín MP, Matheny PB, Nguyen NH, Niskanen T, Oja J, Peay KG, Peintner U, Peterson M, Põldmaa K, Saag L, Saar I, Schüßler A, Scott JA, Senés C, Smith ME, Suija A, Taylor DL, Telleria MT, Weiss M, Larsson KH. 2013. Towards a unified paradigm for sequence-based identification of fungi. Molecular Ecology. 22(21):5271-5277.

Lagueux D, Jumpponen A, Porras-Alfaro A. 2021. Experimental drought re-ordered assemblages of root-associated fungi across North American grasslands. Journal of Ecology. 109:776-792.

Mandyam K, Fox C, Jumpponen A. 2010. Septate endophyte colonization and host responses of grasses and forbs native to a tallgrass prairie. Mycorrhiza. 22:109-119.

O'Donnell K, Sutton DA, Rinaldi MG, Sarver BAJ, Balajee SA, Schroers H, Summerbell RC, Robert VARG, Crous PW, Zhang N, Aoki T, Jung K, Park J, Lee Y, Kang S, Park B, Geiser DM. 2010. Internet-Accessible DNA Sequence Database for Identifying *Fusaria* from Human and Animal Infections. Journal of Clinical Microbiology. 48(10):3708–3718.

OECD (2000a). Guidance Document on Acute Oral Toxicity. Environmental Health and Safety Monograph Series on Testing and Assessment No. 24.

OECD. (2000b). Revised Draft Guidance Document on the Recognition, Assessment and Use of Clinical Signs as Humane Endpoints for Experimental Animals Used in Safety Evaluation.

Rohn H, Junker A, Hartmann A, Grafahrend-Belau E, Treutler H, Klapperstück M, Czauderna T, Klukas C, Schreiber F. 2012. VANTED v2: a framework for systems biology applications. BMC Syst Biol. 6:139.

Rudgers, JA, Fox S, Porras-Alfaro A, Herrera J, Reazin C, Kent DR, Souza L, Chung YA, Jumpponen A. 2022. Biogeography of root-associated fungi in foundation grasses of North American plains. Biogeography. 49:22-37.

Schoch CL, Seifert KA, Huhndorf S. 2012. Nuclear Ribosomal Internal Transcribed Spacer (ITS) Region as a Universal DNA Barcode Marker for Fungi. Proceedings of the National Academy of Sciences. 109(16):6241-6246.

Schüller C, Brewster JL, Alexander MR, Gustin MC, Ruis H. 1994. The HOG pathway controls osmotic regulation of transcription via the stress response element (STRE) of the *Saccharomyces cerevisiae* CTT1 gene. EMBO J. 13(18):4382-4389.

Stojanovski K, Ferrar T, Benisty H, Uschner F, Delgado J, Jimenez J, Solé C, Nadal E, Klipp E, Posas F, Serrano L, Kiel C. 2017. Interaction Dynamics Determine Signaling and Output Pathway Responses. Cell Rep. 19(1):136-149.

Szopinska A, Degand H, Hochstenbach JF, Nader J, Morsomme P. 2011. Rapid response of the yeast plasma membrane proteome to salt stress. Mol. Cell. Proteom. 10:M111.009589.

Tatebayashi K, Yamamoto K, Tomida T, Nishimura A, Takayama T, Oyama M, Kozuka-Hata H, Adachi-Akahane S, Tokunaga Y, Saito H. 2020. Osmostress enhances activating phosphorylation of Hog1 MAP kinase by mono-phosphorylated Pbs2 MAP2K. EMBO Journal. 39:e103444.

Vilgalys R, Hester M. 1990. Rapid genetic identification and mapping enzymatically amplified ribosomal DNA from several *Cryptococcus* species. Journal of Bacteriology 172:4238-4246.

White TJ, Bruns T, Lee S, Taylor J. 1990. Amplification and direct sequencing of fungal ribosomal RNA genes for phylogenetics. In: Innis MA, Gelfand DH, Sninsky JJ, White, TJ, eds. PCR protocols a guide to methods and applications. New York: Academic Press. 1990:315-322.

3. Results & Discussion: ED_{50} and KEGG Pathways

Fungal salt tolerance

We evaluated NaCl-tolerance (ED_{50} – Dixon and Mood 1948; OECD 2000a; OECD 200b) across five ascomycete species of species complexes and compared isolates originating from either arid or mesic sites (MAP < 600 mm or MAP > 600 mm, respectively). Across all thirty isolates included in our analyses, there was no strong evidence for differences in ED_{50} among isolates originating from arid or mesic sites (Mixed Effects ANOVA: $F_{1,264} = 3.27$, $P = 0.0716$) (Fig. 1) suggesting absent general ecotypic adaptation to prevailing environmental conditions, specifically MAP in this case. Although there was no support for general ecotypic adaptation among strains, fungal species varied in their estimated ED_{50} (Mixed Effects ANOVA: $F_{4, 252} = 113.03$, $P < 0.0001$), supporting our first hypothesis, and differed in ED_{50} depending on whether the conspecific isolates had originated from arid or mesic sites as indicated by the interaction between MAP at the origin site and species identity (Mixed Effects ANOVA: $F_{4, 252} = 7.52$, $P < 0.0001$). Again, these analyses provided no strong support for overall differences in ED_{50} for isolates originating from either arid or mesic sites (Mixed Effects ANOVA: $F_{1, 252} = 3.52$, $P = 0.0616$) (Fig. 1).

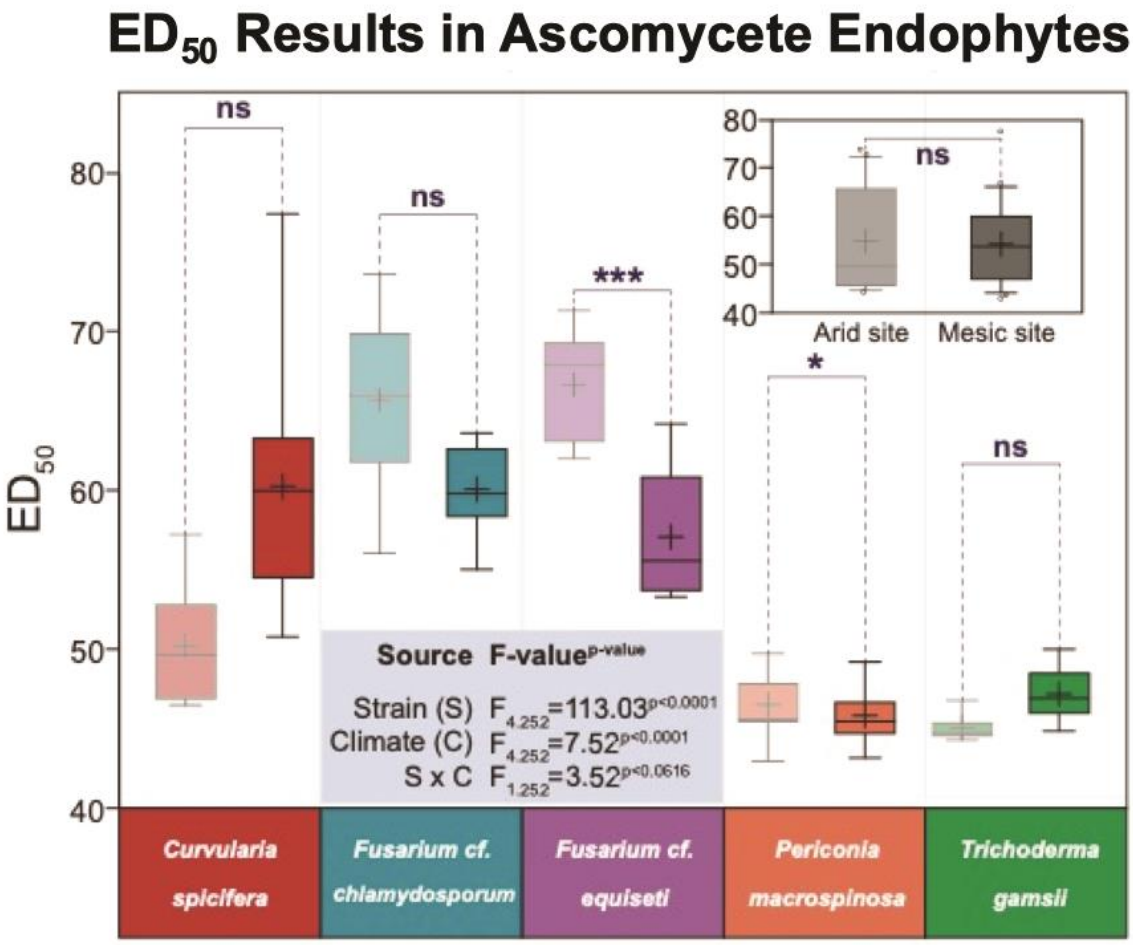

Figure 1. NaCl ED_{50} estimates for root-associated ascomycetes isolated from arid and mesic sites. NaCl ED_{50} estimates (NaCl concentration that reduced terminal colony radius by 50%) are first divided to the five selected ascomycete species and then by site origin from either arid and or mesic sites based on estimated MAP (MAP < 600 mm or MAP > 600 mm, respectively). The inserted figure (top right) shows the relative NaCl ED_{50} of all the isolates divided only to arid and mesic sites based on estimated MAP. Pairwise Comparisons among all included isolates (insert) and within each species are based on one-way ANOVAs and the asterisks and lettering refer to these *P*-values (*** – 0.01 ≤ *P* < 0.05; ** – 0.001 ≤ *P* < 0.01; *** – *P* < 0.001;** ns **– *P* ≥0.05)**.

When isolates from arid and mesic sites were analyzed separately for each species or species complex, isolates representing two of the five species differed based on the MAP at the site of origin (Fig. 1): *Fusarium* cf. *equiseti* complex isolates from arid sites had higher ED_{50} than those from mesic sites (One-Way ANOVA: $F_{1,52} = 23.75$; $P < 0.0001$), whereas *Periconia*

macrospinosa isolates from mesic sites had higher ED_{50} than those from arid sites (One-Way ANOVA: $F_{1,52} = 7.10$; $P = 0.0102$). These analyses further suggest that ecotypic adaptation to prevailing environmental conditions does not exist for the selected taxa and can indeed be opposite to our initial hypotheses. We selected *P. macrospinosa* for our proteomic analyses because of its importance in nutrient-limited ecosystems (Knapp et al. 2018), perceived function in host stress tolerance (Jumpponen 2001), ubiquitous presence and global distribution in grassland systems (Mandyam and Jumpponen 2005), previous examples of reliable ITS barcode-based taxon identification (O'Donnell 2010), and its recently available annotated genome (Knapp et al. 2018).

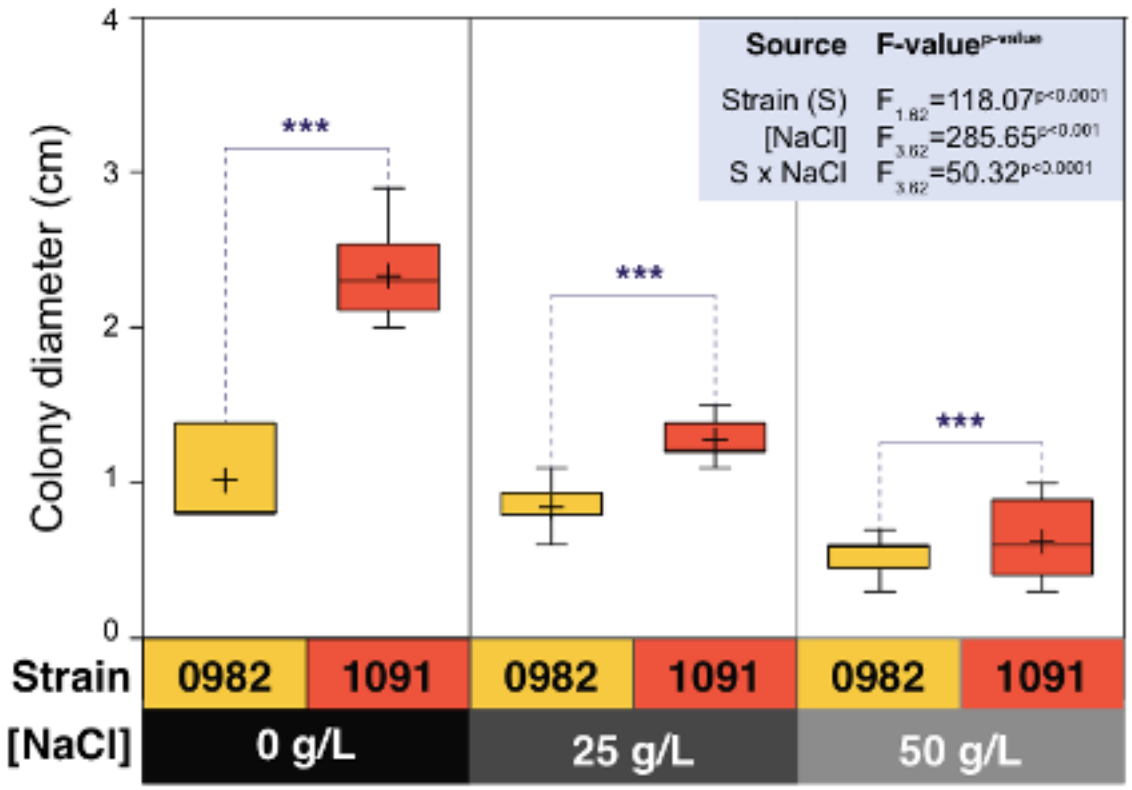

Figure 2. Terminal colony radii of the two *Periconia macrospinosa* isolates under three NaCl concentrations (0g/L, 25g/L, 50g/L); there was no visible growth at the highest NaCl concentration (100g/L). The boxplot shows the terminal colony radii of two *P. macrospinosa*

isolates (high ED_{50} isolate DS 0982 and low ED_{50} isolate DS 1091) selected for the proteomic studies based on their NaCl ED_{50}. Isolates were grown on quad plates for seven days at which point the unamended quadrant's growth reached the plate's edge for the fastest growing isolate. Asterisks above the boxplot represent *P*-values of one-way ANOVAs for the pair of isolates under that NaCl concentration (*** – 0.01 ≤ P < 0.05; ** – 0.001 ≤ P < 0.01; *** – P < 0.001;** ns – **P ≥0.05**).

We selected two *P. macrospinosa* isolates – DS 0982 (mesic site, high ED_{50}) and DS 1091 (arid site, low ED_{50}) – with the most extreme ED_{50} estimates for proteomic analyses. The terminal colony radius measured after seven days in NaCl challenges varied between the two strains depending on the NaCl concentration as indicated by the strain x [NaCl] interaction (Mixed Effects ANOVA: $F_{3,62} = 50.32$; $P < 0.0001$) (Fig. 2). The two strains differed in growth (Mixed Effects ANOVA: $F_{1,62} = 118.07$; $P < 0.0001$) and the increase in [NaCl] reduced growth (Mixed Effects ANOVA: $F_{3,62} = 285.65$; $P < 0.0001$). The interaction effect was mainly attributable to the minimal decline in the growth of the slower growing strain from the mesic site (DS 0982) with higher ED_{50} (Fig. 2). These data highlight the higher ED_{50} and minimal growth response to salinity in DS 0982 and the lower ED_{50} and greater reduction in growth in response to salinity in DS 1091.

Condition-dependent proteomic profiling of *P. macrospinosa*

We hypothesized that, due to MAP of site origin, the isolate from the more arid environment, DS 1091, would demonstrate greater resistance to salt through a greater abundance of proteins associated with salt-tolerating strategies. Contrary to our hypothesis, growth of DS 1091, the isolate originating from a dryer environment, declined rapidly in response to salinity. Based on the differences in growth responses to increasing NaCl concentration, we hypothesized that DS 1091, the fast-growing isolate with low ED_{50} and greater decline in growth, would show greater proteomic responses to salinity than the slow growing DS 0982 with high ED_{50}. Our

proteomic analysis yielded a total of 4,749 individual *P. macrospinosa* proteins (Table S3). To categorize and compare proteomic data associated with specific pathways, we utilized a GhostKoala orthologous GhostX search and KEGG annotation as described in Kanehisa et al. (2016). The proteome data indicated that the two strains substantially differed in their response to NaCl stress. Additionally, these data suggest strong metabolic responses as well as changes in cell wall and plasma membrane synthesis. Further, these analyses provide evidence for activation and interaction of the HOG pathway in response to salinity.

KEGG Pathway Enrichment Analysis

We identified the responses of proteins associated with specific pathways using a KEGG pathway enrichment analysis (Fig. 3). We used k-means clustering, which identified a total of five major clusters demonstrating differences in protein abundances between the isolates and in their responses to salinity. Overall, we identified a total of 112 enriched KEGG pathways, including key pathways involved in fundamental and basic cellular metabolism such as glycolysis and the TCA cycle.

Fungal adaptive responses to salinity often occur through signal transduction mechanisms which result in the restructuring of the fungal cell wall (Alex et al. 1996; Schumacher et al. 1997; Zhang et al. 2010; Hagiwara et al. 2013; Perez-Nadales et al. 2015; Ene et al. 2015), composition amendments to the cell membrane (Petrovič et al. 2002; Turk et al. 2004; Gunde-Cimerman et al. 2007; Manzanares-Estreder et al. 2017a; Manzanares-Estreder et al. 2017b; Pascual-Ahuir et al. 2017) and/or the accumulation and regulation of intracellular osmolytes (Albertyn et al. 1994; Luyten et al. 1995; San José et al. 1996; Hohmann 1997; Kirk 1997; Sutherland et al. 1997; Rep et al. 1999; Hohmann et al. 2002; Kayingo and Wong 2005; Klipp et al. 2005; Ashraf and Foolad

2007; Hohmann et al. 2007; Saito and Posas 2012; Lee et al. 2013; Pérez-Llano et al. 2020). Our data are consistent with these reports and highlight upregulation of mechanisms involved in cell wall remodeling, plasma membrane configuration, and osmolyte regulation in response to salt.

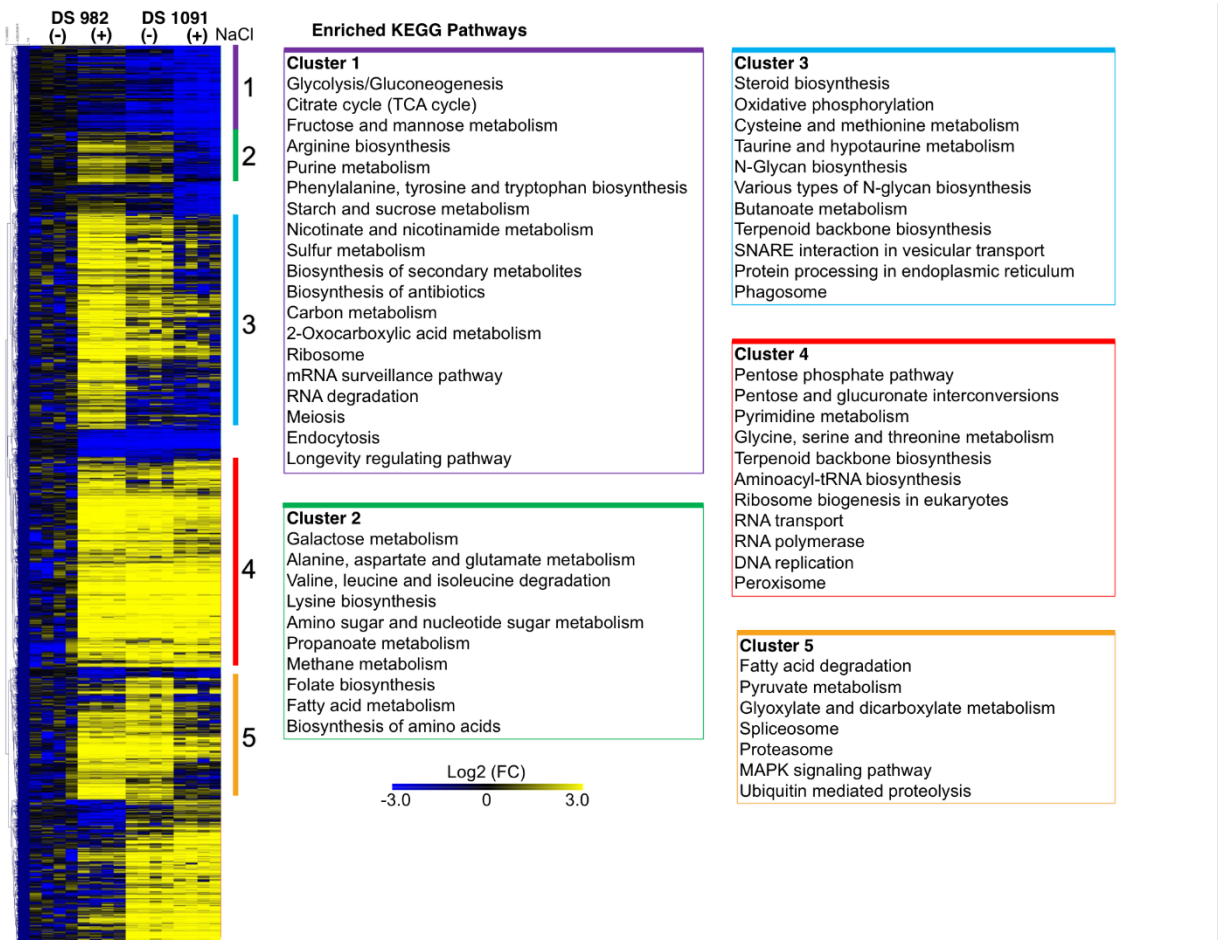

Figure 3. Heat map of protein abundances in enriched KEGG pathways of two *P. macrospinosa* isolates (slow-growing, high-ED$_{50}$ isolate DS 0982 and fast-growing, low-ED$_{50}$ isolate DS 1091) with (+) and without (–) salt stress. Proteins are listed in the heatmap and separated by isolate and [NaCl] condition with enriched KEGG pathways separated into five k-means clusters based on the protein abundance between the four combinations of *P. macrospinosa* isolates and [NaCl] conditions. The complete list of proteins, their relative abundances, and *P*-values (determined by *t*-test) are listed in Supplemental Table S3. A complete list of KEGG enriched pathways and k-mean separated clusters is available in Supplemental Table S4.

K-means clustering revealed dramatic differences in protein abundances between and within the two *P. macrospinosa* isolates, apparent in comparisons of both control conditions and prolonged salinity stress. Consistent with our hypotheses, the two isolates differed in the enrichment of several pathways including those relevant to cell wall restructuring, cell membrane reorganization, and osmolyte regulation including steroid biosynthesis, fatty acid metabolism, and the MAPK signaling pathway.

Cluster 1 in Fig. 3 highlights a trend of downregulation, in response to NaCl stress, of critical KEGG pathways associated with glycolysis, the TCA cycle, and several specific cell metabolisms, particularly in the fast-growing, low-ED_{50} isolate DS 1091, whose growth declined rapidly with increasing NaCl concentration. The observed downregulation of general cell metabolism to generate cellular energy in the isolate with low ED_{50} is consistent with its observed growth decline in response to prolonged salt stress and the rapid decline in its growth in response to increasing [NaCl]. Further, this downregulation of critical pathways is likely a result of targeted cellular investment to pathways and processes related osmoadaptive responses.

Cluster 2 in Fig. 3 highlights the upregulation in the slow growing strain DS 0982 with high ED_{50} and an inverse downregulation in DS 1091 in response to salinity, conspicuously in galactose metabolism and also in several regulatory pathways involved in the metabolism and biosynthesis of amino acids. Galactose metabolism results in glucose 6-phosphate (G6P), a cell membrane impermeable compound which accumulates in the cytosol and is required as an upstream biomolecule in glycerol production (Wang et al. 2001). While DS 0982 demonstrated an increase in G6P in response to salinity, indicating potential glycerol and glucose production – DS 1091 appears to have an inverse response. This, coupled with the evident downregulation of the TCA cycle in DS 1091 in response to salinity, provides further evidence for regulatory

responses to osmotic stress, with DS 0982 maintaining growth and metabolic activity toward survival efforts against salt challenge and DS 1091 evidently losing basic cellular function. Considering the indirect connection between galactose metabolism providing an upstream molecule for glycerol production and the TCA cycle's direct effect on glycolysis, DS 1091 appears to downregulate and disinvest its regulatory efforts, whereas DS 0982 upregulates metabolism efforts in response to salt – potentially related to regulatory effects on glycolysis and likely aiding in an increase in cytosolic glycerol as a non-toxic intracellular regulator (Dihazi et al. 2004). This is especially important because among all osmoadaptive responses, the production and accumulation of glycerol in the cytoplasm is critical for successful osmoadaptation (Babazadeh et al. 2014). The several pathway responses related to amino acid metabolism apparent in cluster 2 also suggest potential recycling of transcriptional subunits relating to changes in expression in response to salinity within the slow-growing DS 0982 isolate. Similar to cluster 2, the salinity response of the two isolates tends to be inverse in cluster 3.

Cluster 3 suggests strong inverse responses in isolates with an upregulation in DS 0982 and a downregulation in DS 1091 in steroid biosynthesis, N-glycan biosynthesis, and oxidative phosphorylation as well as vesicular transport and protein processing. Taken together, these likely indicate potential cell membrane amendments in the slow growing isolate DS 0982 in response to salt stress through steroid synthesis (Nes et al. 1989; Kristan and Rižner 2012; Hu et al. 2017) especially biosynthesis of ergosterol (Rodrigues 2018), a key membrane sterol that regulates membrane fluidity. In conjunction, potential cell wall strengthening may have simultaneously occurred via N-glycan biosynthesis in DS 0982. This not only suggests further amendment to the cell membrane via N-glycosated and membrane-anchored extracellular

glycans but also implies cell wall strengthening via cell wall glycan cross-linkages (Doering et al. 2017) and enforces responsive regulation in intracellular transport, secretion, and defense against proteolytic degradation (Dos Reis Almeida et al. 2011). N-glycans pre-assemble to cell membrane anchors before being further processed in the endoplasmic reticulum – Golgi pathway, further supporting the enrichment of protein processing KEGG pathway in DS 0982. A final note in cluster 3 is the upregulation of oxidative phosphorylation in DS 0982 and its downregulation in DS 1091. Consistent with the above findings, oxidative phosphorylation generates ATP for cellular energy, confirming that the slow-growing DS 0982 isolate is adapting to and surviving in the salt-laden substrate whereas the fast-growing DS 1091 isolate is shutting down key metabolic functions necessary to sustain growth.

Another major challenge is the osmotic stress that directly results from salt stress. Osmotic stress increases intracellular and extracellular oxidative stress contributors such as reactive-oxygen species (ROS), which react with protein substrates inactivating functional intracellular components (Breitenbach et al. 2015) and may even extracellularly enact changes and restructuring within the cell wall (Podgórska et al. 2017). Coordinating with the alleged upregulation of transmembrane transport and secretion implied by the enrichment of N-glycan biosynthesis, another transport pathway – vesicular transport – was also enriched in DS 0982 and comparatively downregulated in DS 1091 (Fig. 3). The underlying mechanisms of these transport schemes suggest the translocation of ROS from the cytoplasm. ROS transport to the extracellular space may relieve intracellular oxidative stress, permit protein function maintenance, and interact to support the cell wall remodeling (Podgórska et al. 2017). Earlier research suggests that oxidative stress inhibits vesicle trafficking from the cytosol to the plasma membrane in the model yeast *S. cerevisiae* (Mazel et al. 2004). Some intracellular proteins which ROS molecules

inactivate are critical for energy production, such as G6P, through the pentose phosphate pathway (Lushchak and Gospodaryov 2005) and could elucidate the loss of normal function and metabolic maintenance - leaving DS 1091 unable to cope and maintain activity in response to salt.

The extracellular relocation of ROS by both vesicular transport and N-glycan related secretory mechanisms also indicate cellular maintenance and energy conservation via ROS export to counteract the potential damage from increase in intracellular ROS caused by osmotic stress (Heinisch et al. 2020). Following this logic, the slow-growing, high-ED_{50} DS 0982 isolate likely responds to mild salinity by exploiting a cellular preservation through membrane modifications, cell wall reinforcement, critical resource production, and conservation and allotment of cellular energy necessary for membrane and cell wall restructuring.

Cluster 4 confirms the increase in overall protein abundance in DS 0982 in response to salt and a consistent, relative to the overall stable protein abundance in the fast-growing, low-ED_{50} DS 1091 isolate. This cluster highlights differences in the adaptive response such that DS 0982 responds to osmotic stress with upregulation, whereas DS 1091 does not respond strongly in protein quantity. Major KEGG pathways in cluster 4 that were upregulated in DS 0982 in response to salt include the pentose phosphate pathway, ribosome biogenesis, RNA polymerase, and terpenoid backbone biosynthesis. Consistent with cluster 3 and the protective strategy of removing excess ROS to prevent inhibition of the pentose phosphate pathway, the enrichment of pentose phosphate pathway highlights the upregulation of a key pathway in cellular energy production. The upregulation of these pathways suggests that DS 0982 increased its cellular activity in response to salinity and provides support for cellular investment in transcription, most likely to assist in cell wall and plasma membrane reorganization and restructuring to counteract

osmotic stressors. In further support, the enriched terpenoid backbone biosynthesis pathway similarly suggests downstream cell membrane modification, as this pathway acts as an upstream regulator for biosynthesis of ergosterol, an essential structural component in fungal cell membranes (Wang et al. 2019). In contrast, the fast-growing DS 1091 isolate seems to downregulate efforts to maintain and modify cell membranes and cell walls, indicating its inability to counteract the increased salinity, perhaps in an effort to aid in its survival as the colony begins to shut down cellular operations.

Similar to clusters 2 and 3, cluster 5 shows contrasting responses to salinity between the two isolates. The enriched pathways in cluster 5 include fatty acid degradation, pyruvate metabolism, and mitogen-activated protein kinase (MAPK) signaling pathways. Fatty acid degradation pathway upregulation in the slow-growing DS 0982 isolate in response to salt suggests membrane reformation through the breakdown of fatty acids – critical subunits of membrane sterols and phospholipids which themselves contribute to membrane rigidity (Pan et al. 2018). This is consistent with the observed upregulation of upstream factors of ergosterol biosynthesis (cluster 4) and provides further evidence for the conceivable restructuring of plasma membrane constituents via recycling and interactions with fatty acid dependent membrane components. This fatty acid repurposing may also aid in cellular defense responses against saline stress through its action as an intracellular signal transducer (Duplus et al. 2000). In line with this, this response may constitute a metabolic shift in response to salinity, perhaps through peroxisomal assisted degradation (Pascual-Ahuir et al. 2018). Consistently, upregulation of the pyruvate metabolism pathway in DS 0982 indicates a downstream effect and subsequent upregulation of both fatty acid and ergosterol biosynthesis, both of which contribute to fungal cell membrane organization (Rodrigues 2018; Zamith-Miranda et al. 2019). In consistent

contrast with DS 0982, the fast-growing DS 1091 appears to downregulate fatty acid degradation, suggesting its disinvestment in membrane maintenance and pyruvate metabolism. Taken together, this indicates a further downregulation of fatty acid and ergosterol biosynthesis. These data suggest that the fast-growing DS 1091 isolate is not investing in conservative tactics such as metabolism maintenance or cell remodeling, whereas the slow-growing DS 0982 isolate is.

Cluster 5 highlighted responses in the MAPK signaling pathway. Perhaps the most informative and interesting within this pathway is the high-osmolarity glycerol (HOG) pathway. The MAPK signaling pathway is imperative for many cellular responses to extracellular stimuli (Bahn et al. 2007; Román et al. 2020) because it is central in regulating transcription factors. Transcription factors affect critical fungal functions including cell cycle regulation and hyphal growth (Carbó and Pérez-Martín 2010; Correia et al. 2010; Chen et al. 2020), cell differentiation and morphogenesis (Martínez-Soto and Ruiz-Herrera 2017; Román et al. 2005), cell wall assembly and integrity (Jiménez-Gutiérrez et al. 2020; Dichtl et al. 2016), and cellular stress responses (Hagiwara et al. 2016). However, MAPK regulated HOG directly and specifically relates to fungal responses to saline and osmotic stresses (Konte et al. 2016). This histidine-kinase pathway regulates salt stress and salt-induced osmotic stress through the production and accumulation of compatible osmolytes, predominantly glycerol (Kayingo and Wong 2005). Overall, our proteomic data provide evidence for fundamental changes in the cellular metabolism, the structure and integrity of the fungal cell wall and plasma membrane, as well as the employment and interaction of the HOG pathway in response to NaCl-induced salinity and osmotic stresses. We discuss the cell wall and plasma membrane modifications in the subsequent sections and specifically discuss the evidence for the HOG pathway in *P. macrospinosa.*

References

Albertyn J, Hohmann S, Thevelein JM, Prior BA. 1994. GPD1, which encodes glycerol-3-phosphate dehydrogenase, is essential for growth under osmotic stress in saccharomyces cerevisiae, and its expression is regulated by the high-osmolarity glycerol response pathway Mol. Cell. Biol. 14(6):4135-4144

Alex LA, Borkovich KA, Simon MI. 1996. Hyphal development in *Neurospora crassa*: involvement of a two-component histidine kinase. Proc Natl Acad Sci. 93(8):3416-3421.

Ashraf M and Foolad MR. 2007. Roles of glycine betaine and proline in improving plant abiotic stress resistance. Environ Exp Bot. 59:207–216.

Babazadeh R, Furukawa T, Hohmann S, Furukawa K. 2014. Rewiring yeast osmostress signalling through the MAPK network reveals essential and non-essential roles of Hog1 in osmoadaptation. Sci. Rep. 4:4697.

Bahn YS, Xue C, Idnurm A, Rutherford JC, Heitman J, Cardenas ME. 2007. Sensing the environment: lessons from fungi. Nat Rev Microbiol. 5:57-69.

Breitenbach M, Weber M, Rinnerthaler M, Karl T, Breitenbach-Koller L. 2015. Oxidative stress in fungi: its function in signal transduction, interaction with plant hosts, and lignocellulose degradation. Biomolecules. 5(2):318-342.

Carbó N and Pérez-Martín J. 2010. Activation of the Cell Wall Integrity Pathway Promotes Escape from G2 in the Fungus Ustilago maydis. PLoS Genet 6(7):e1001009.

Chen H, Zhou X, Ren B, Cheng L. 2020. The regulation of hyphae growth in *Candida albicans*. Virulence 11(1):337-348.

Correia I, Alonso-Monge R, Pla J. 2010. MAPK cell-cycle regulation in Saccharomyces cerevisiae and Candida albicans. Future Microbiol 5(7):1125-41.

Dichtl K, Samantaray S, and Wagener J. 2016. Cell wall integrity signaling in human pathogenic fungi. Cellular Microbiology 18:1228-1238.

Dihazi H, Kessler R, Eschrich K. 2004. High Osmolarity Glycerol (HOG) Pathway-induced Phosphorylation and Activation of 6-Phosphofructo-2-kinase Are Essential for Glycerol Accumulation and Yeast Cell Proliferation under Hyperosmotic Stress*. Journal of Biological Chemistry. 279(23):23961-23968.

Dixon WJ and Mood AM. 1948. A Method for Obtaining and Analyzing Sensitivity Data. Journal of American Statistics Association. 43:109-126.

Doering TL, Cummings RD, Aebi M. Fungi. 2017. In: Varki A, Cummings RD, Esko JD, Stanley P, Hart GW, Aebi M, Darvill AG, Kinoshita T, Packer NH, Prestegard JH,

Schnaar RL, Seeberger PH, editors. Essentials of Glycobiology. 3rd ed. Cold Spring Harbor (NY): Cold Spring Harbor Laboratory Press; 2015–2017. Chapter 23.

Dos Reis Almeida FB, Carvalho FC, Mariano VS, Alegre ACP, Silva RdN, Hanna ES, Roque-Barreira MC. 2011. Influence of N-Glycosylation on the Morphogenesis and Growth of *Paracoccidioides brasiliensis* and on the Biological Activities of Yeast Proteins. PLoS ONE. 6(12):e29216.

Duplus E, Glorian M, Forest C. 2000. Fatty acid regulation of gene transcription. J Biol Chem. 275(40):30749-30752.

Ene IV, Walker LA, Schiavone M, Lee KK, Martin-Yken H, Dague E, Gow NAR, Munro CA, Brown AJ. 2015. Cell wall remodeling enzymes modulate fungal cell wall elasticity and osmotic stress resistance. mBio. 6(4):e00986.

Gunde-Cimerman N, Turk M, Abramovi Z, Plemenitaš A. 2007. Salt stress and plasma-membrane fluidity in selected extremophilic yeasts and yeast-like fungi. FEMS Yeast Res. 7:550-557.

Hagiwara D, Sakamoto K, Abe K, Gomi K. 2016. Signaling pathways for stress responses and adaptation in *Aspergillus* species: stress biology in the post-genomic era. Biosci Biotechnol Biochem. 80:1667-1680.

Hagiwara D, Yoshimi A, Sakamoto K, Gomi K, Abe K. 2015. Response and adaptation to cell wall stress and osmotic stress in *Aspergillus* species. Stress Biology of Yeasts and Fungi. Tokyo: Springer Japan. 2015:199–218.

Hohmann S, Krantz M, Nordlander B. 2007. Yeast osmoregulation. Methods Enzymol. 428:29-45.

Hohmann S. 1997. Shaping up: the response of yeast to osmotic stress. In: Hohmann S, Mager WH, eds. Yeast stress responses. R.G. Landes, Austin, Texas. 1997:101–145.

Hohmann S. 2002. Osmotic adaptation in yeast--control of the yeast osmolyte system. Int Rev Cytol. 215:149-187.

Hu Z, He B, Ma L, Sun Y, Niu Y, Zeng B. 2017. Recent Advances in Ergosterol Biosynthesis and Regulation Mechanisms in *Saccharomyces cerevisiae*. Indian J Microbiol. 57(3):270-277.

Jiménez-Gutiérrez E, Alegría-Carrasco E, Alonso-Rodríguez E, Fernández-Acero T, Molina M, Martín H. 2020. Rewiring the yeast cell wall integrity (CWI) pathway through a synthetic positive feedback circuit unveils a novel role for the MAPKKK Ssk2 in CWI pathway activation. FEBS J. 287(22):4881-4901.

Jumpponen A. 2001. Dark septate endophytes-are they mycorrhizal?. Mycorrhiza. 11:207-211.

Kanehisa M, Sato Y, Morishima K. 2016. BlastKOALA and GhostKOALA: KEGG Tools for Functional Characterization of Genome and Metagenome Sequences. J Mol Biol. 428(4):726-731.

Kayingo G and Wong B. 2005. The MAP kinase Hog1p differentially regulates stress-induced production and accumulation of glycerol and D-arabitol in *Candida albicans*. Microbiology. 151(9):2987-2999.

Kirk K. 1997. Swelling-activated organic osmolyte channels. J Membr Biol. 158:1-16.

Klipp E, Nordlander B, Krüger R, Gennemark P, Hohmann S. 2005. Integrative model of the response of yeast to osmotic shock. Nat Biotechnol. 23(8):975-982.

Knapp DG, Németh JB, Barry K, Hainaut M, Henrissat B, Johnson J, Kuo A, Lim JHP, Lipzen A, Nolan M, Ohm RA, Tamás L, Grigoriev IV, Spatafora JW, Nagy LG, Kovács GM. 2018. Comparative genomics provides insights into the lifestyle and reveals functional heterogeneity of dark septate endophytic fungi. Sci Rep. 8(1):6321.

Konte T, Terpitz U, Plemenitaš A. 2016. Reconstruction of the High-Osmolarity Glycerol (HOG) Signaling Pathway from the Halophilic Fungus *Wallemia ichthyophaga* in Saccharomyces cerevisiae. Front. Microbiol. 7:901.

Kristan K and Rižner TL. 2012. Steroid-transforming enzymes in fungi. The Journal of Steroid Biochemistry and Molecular Biology. 129(2):79-91.

Lee J, Reiter W, Dohnal I, Gregori C, Beese-Sims S, Kuchler K, Ammerer G, Levin DE. 2013. MAPK Hog1 closes the *S. cerevisiae* glycerol channel Fps1 by phosphorylating and displacing its positive regulators. Genes Dev. 27(23):2590-2601.

Lushchak VI and Gospodaryov DV. 2005. Catalases protect cellular proteins from oxidative modification in Saccharomyces cerevisiae. Cell Biol Int. 29(3):187-192.

Luyten K, Albertyn J, Skibbe WF, Prior BA, Ramos J, Thevelein JM, Hohmann S. 1995. Fps1, a yeast member of the MIP family of channel proteins, is a facilitator for glycerol uptake and efflux and is inactive under osmotic stress. EMBO J. 14(7):1360-1371.

Mandyam K, Jumpponen A. 2005. Seeking the elusive function of the root-colonising dark septate endophytic fungi. Stud. Mycol. 53:173–189.

Manzanares-Estreder S, Espí-Bardisa J, Alarcón B, Pascual-Ahuir A, Proft M. 2017b. Multilayered control of peroxisomal activity upon salt stress in *Saccharomyces cerevisiae*. Mol Microbiol. 104(5):851-868.

Manzanares-Estreder S, Pascual-Ahuir A, Proft M. 2017a. Stress-activated degradation of sphingolipids regulates mitochondrial function and cell death in yeast. Oxidative Med Cell Longev. 2017:1–14.

Martínez-Soto D, Ruiz-Herrera J. 2017. Functional analysis of the MAPK pathways in fungi. Revista Iberoamericana de Micologia 34(4):11301406.

Mazel A, Leshem Y, Tiwari BS, Levine A. 2004. Induction of salt and osmotic stress tolerance by overexpression of an intracellular vesicle trafficking protein AtRab7 (AtRabG3e). Plant Physiol. 134(1):118-128.

Nes WD, Xu S, Haddon WF. 1989. Evidence for similarities and differences in the biosynthesis of fungal sterols. Steroids. 53(5):533-558.

O'Donnell K, Sutton DA, Rinaldi MG, Sarver BAJ, Balajee SA, Schroers H, Summerbell RC, Robert VARG, Crous PW, Zhang N, Aoki T, Jung K, Park J, Lee Y, Kang S, Park B, Geiser DM. 2010. Internet-Accessible DNA Sequence Database for Identifying *Fusaria* from Human and Animal Infections. Journal of Clinical Microbiology. 48(10):3708–3718.

OECD (2000a). Guidance Document on Acute Oral Toxicity. Environmental Health and Safety Monograph Series on Testing and Assessment No. 24.

OECD. (2000b). Revised Draft Guidance Document on the Recognition, Assessment and Use of Clinical Signs as Humane Endpoints for Experimental Animals Used in Safety Evaluation.

Pan J, Hu C, Yu JH. 2018. Lipid Biosynthesis as an Antifungal Target. J Fungi (Basel). 4(2):50.

Pascual-Ahuir A, Manzanares-Estreder S, Timón-Gómez A, Proft M. 2018. Ask yeast how to burn your fats: lessons learned from the metabolic adaptation to salt stress. Curr Genet. 64:63–69.

Pérez-Llano Y, Rodríguez-Pupo EC, Druzhinina IS, Chenthamara K, Cai F, Gunde-Cimerman N, Zalar P, Gostinčar C, Kostanjšek R, Folch-Mallol JL, Batista-García RA, Sánchez-Carbente MdR. 2020. Stress Reshapes the Physiological Response of Halophile Fungi to Salinity. Cells. 9(3):525.

Perez-Nadales E and Di Pietro A. 2015. The transmembrane protein Sho1 cooperates with mucin Msb2 to regulate invasive growth and plant infection in *Fusarium oxysporum*. Mol Plant Pathol. 16:593–603.

Petrovič U, Gunde-Cimerman N, Plemenitaš A. 2002. Cellular responses to environmental salinity in the halophilic black yeast *Hortaea werneckii*. Molecular Microbiology. 45:665-672.

Podgórska A, Burian M, Szal B. 2017. Extra-Cellular But Extra-Ordinarily Important for Cells: Apoplastic Reactive Oxygen Species Metabolism. Front Plant Sci. 8:1353.

Rodrigues ML. 2018. The multifunctional fungal ergosterol. mBio. 9:e01755-18.

Román E, Correia I, Prieto D, Alonso R, and Pla, J. 2020. The HOG MAPK pathway in *Candida albicans*: more than an osmosensing pathway. International Microbiology. 23(1):23-29.

Román E, Nombela, C, and Pla, J. 2005. The Sho1 Adaptor Protein Links Oxidative Stress to Morphogenesis and Cell Wall Biosynthesis in the Fungal Pathogen Candida Albicans. Molecular and Cellular Biology 25.23:10611-0627.

Saito H and Posas F. 2012. Response to hyperosmotic stress. Genetics. 192(2):289-318.

San José C, Monge RA, Pérez-Díaz R, Pla J, Nombela C. 1996. The mitogen-activated protein kinase homolog HOG1 gene controls glycerol accumulation in the pathogenic fungus *Candida albicans*. J. Bacterial. 178(19):5850-5852

Schumacher M, Enderlin C, Selitrennikoff C. 1997. The Osmotic-1 Locus of *Neurospora crassa* Encodes a Putative Histidine Kinase Similar to Osmosensors of Bacteria and Yeast. Curr Microbiol. 34:340–347.

Sutherland FCW, Lages F, Lucas C, Luyten K, Albertyn J, Hohmann S, Prior BA, Kilian SG. 1997. Characteristics of FPS1-dependent and –independent glycerol transport in *Saccharomyces cerevisiae*. J Bacteriol 179:7790–7795.

Turk M, Mejanelle L, Sentjur M, Gunde-Cimerman N, Grimalt J, Plemenitaš, A. 2004. Salt-induced changes in lipid composition and membrane fluidity of halophilic yeast-like melanized fungi. Extremophiles. 8:53–61

Wang R, Ma P, Li C. 2019. Combining transcriptomics and metabolomics to reveal the underlying molecular mechanism of ergosterol biosynthesis during the fruiting process of *Flammulina velutipes*. *BMC Genomics* 20:999.

Wang ZX, Zhuge J, Fang H, Prior BA. 2001. Glycerol production by microbial fermentation: a review. Biotechnol Adv. 19(3):201-223.

Zamith-Miranda D, Heyman HM, Cleare LG, Couvillion SP, Clair GC, Bredeweg EL, Gacser A, Nimrichter L, Nakayasu ES, Nosanchuk JD. 2019. Multi-omics Signature of Candida auris, an Emerging and Multidrug-Resistant Pathogen. mSystems. 4(4):e00257-19.

Zhang, H, Liu K, Zhang X, Song W, Zhao Q, Dong Y, Guo M, Zheng X, Zhang Z. 2010. A two-component histidine kinase, MoSLN1, is required for cell wall integrity and pathogenicity of the rice blast fungus, Magnaporthe oryzae. Curr Genet. 56:517–528.

4. Results & Discussion: Cell Wall and Cell Membrane Response to Salinity

Cell Wall Associated Proteomic Responses in *P. macrospinosa*

Before an extracellular stimulus, *e.g.,* increased extracellular salinity, can initiate signaling response in a cell, it must pass the initial fungal barrier – the cell wall. The fungal cell wall is critical for cellular structure and defenses (Hopke et al. 2018). It also mediates cellular interactions with the extracellular environment (Bahn et al. 2007; Román et al. 2020), actively controlling permeability to protect the cell against changing or unfavorable environmental conditions (Gow et al. 2017). During a hyperosmotic shock (high osmolarity conditions caused by high ion concentration) fungal cells lose turgor pressure because the greater ionic concentration gradient initiates responses (Babazadeh et al. 2014) and attempts to achieve homeostatic balancing through cell wall restructuring (Hagiwara et al. 2015), structural and functional reformation of the cell membrane (Gostinčar et al. 2011; Pascual-Ahuir et al. 2018), and compatible osmolyte (e.g., glycerol) accumulation (Klein et al. 2016). The fungal cell wall is composed of a complex, interconnected, and interlinked framework of β-glucans (β-1,3-glucans and β-1,6-glucans) and chitins that provide structural rigidity and tensile strength (Ene et al. 2015).

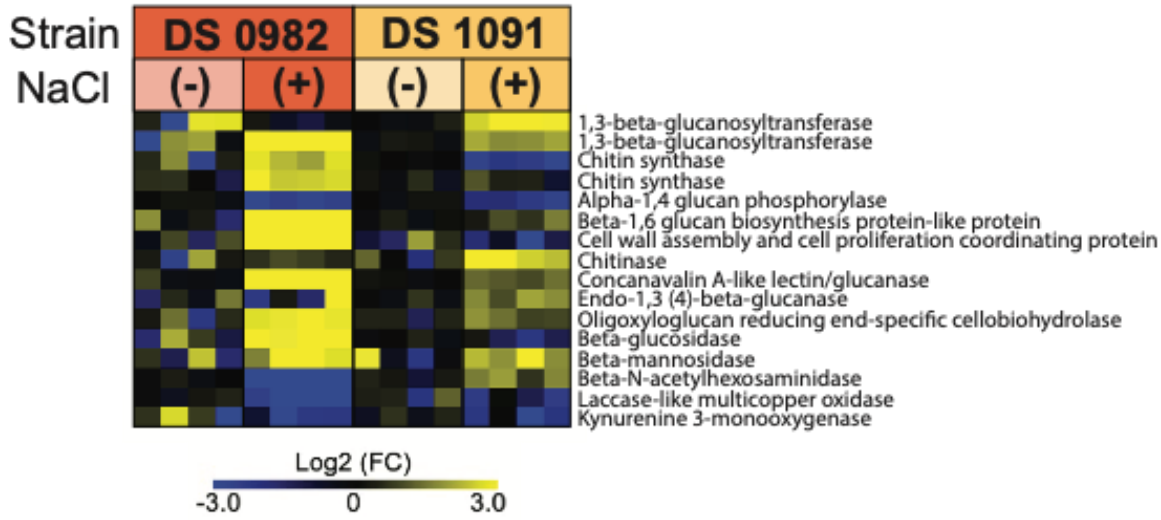

Figure 4. Cell Wall Proteomic Responses of two *P. macrospinosa* isolates (slow-growing, high-ED$_{50}$ isolate DS 0982 and fast-growing, low-ED$_{50}$ isolate DS 1091) to NaCl. Select cell wall protein abundances are shown in the heatmap and separated by isolate and [NaCl]. A complete list of select relevant lipid proteins and their abundances are shown in Supplemental Table S6.

The β-glucans form an interlocking matrix with β-1,3-glucans act as the major cell wall structural component (Fesel and Zuccaro 2016). They form a barrier surrounding the outer plasma membrane where membrane localized chitins covalently bond and support the β-1,3-glucan envelope (Kollár et al. 1995) linking it to the plasma membrane and forming the glucan-chitin structural exoskeleton (Klis et al. 2001). The glucan-chitin exoskeleton is a well-conserved, cross-linked innermost layer of the cell wall assembled by membrane-bound synthases (Latgé 2007). Similar to the lignocellulosic plant cell walls, fungi depend on their glucan-chitin reinforced cell walls for essential structural support and defense against membrane rupture in the case of imbalance in the osmotic pressure gradient (Bowman and Free 2006). The chitin cross-linked β-1,3-glucans provide a strong casing to regulate cell shape and volume – a strategy that functionally dictates growth via turgor pressure in filamentous fungi, such as *P. macrospinosa* (Bartnicki-Garcia et al. 2000). Another important cell wall component is the β-1,6-glucan, which also cross-links with the structurally important β-1,3-glucans (Garcia-Rubio et

al. 2020), contributes to strength and support within the cell wall matrix, and provides a linkage between skeletal β-1,3-glucans and polysaccharide or glycoprotein cell wall proteins, all of which are regulated by and involved in signal transduction (Free 2013; Muszewska et al. 2018).

Our two *P. macrospinosa* isolates shared some responses to salt stress and differed in others. The 1,3-betaglucanosyltransferase was upregulated in both *P. macrospinosa* isolates in response to salt (Fig. 4). The 1,3-betaglucanosyltransferase has been observed in several fungal species and has previously been isolated from an *Aspergillus fumigatus* cell wall autolysate (Okada et al. 1998). It is responsible for commencing β-1,6-glucan inter-linkage to structural cell wall β-1,3-glucans (Mouyna et al. 2005). In contrast to the 1,3-betaglucanosyltransferase that was consistently upregulated in both isolates, chitinase and chitin synthase responses were inverse in the two isolates (Fig. 4). Unlike 1,3-betaglucanosyltransferase, which adds to the cell wall matrix and increases its rigidity, chitinase degrades chitin in the innermost glucan-chitin exoskeleton (Roncero et al. 2020) and plays a role in softening and remolding fungal cell walls. Chitin synthases, in contrast to chitinases, produce chitin (Li et al. 2016), contributing to cell wall structure and strengthening of cell walls in response to salinity.

In the high ED_{50} isolate DS 0982, chitinase downregulation was coupled with chitin synthase upregulation, both key proteins involved in the degradation and synthesis of cellular chitin, cell viability, and cell wall integrity (Shaw et al. 1991; Munro et al. 2001). Chitinase is often a membrane-anchored cell wall associate which acts to degrade cell wall chitins and regulates fungal growth and morphogenesis (Takaya et al. 1998; Adams 2004). Its downregulation and concomitant chitin synthase upregulation suggest cell wall modifications toward stronger, more rigid cell walls in DS 0982 and an inverse response in DS 1091. It should be noted however, that as fungal cell walls mature, chitin continues to covalently cross-link with

β-1,6-glucans and β-1,3-glucans increasing chitin resistance to chitinase degradation (Hartland et al. 1994; Kollár et al. 1997). In contrast to slow-growing, high-ED_{50} isolate, chitinase upregulation was coupled with chitin synthase downregulation in the low-ED_{50} isolate DS 1091, highlighting the opposite NaCl stress responses of the two isolates and suggesting degradative modification leading to cell wall breakdown and increased elasticity in the latter isolate. Based on the chitinase and chitin synthase abundances, we suggest that the slow-growing, high-ED_{50} isolate DS 0982 is increasing the rigidity and strength of its cell wall in response to prolonged NaCl stress, whereas the fast-growing, low-ED_{50} isolate DS 1091 is decreasing rigidity and increasing elasticity of the cell wall. Based on these observations, we posit that salinity drives an adaptive response and results in modification of the cell wall structure in our isolates, albeit in opposite ways.

As further evidence for saline mediated cell wall modification and reinforcement in the high-ED_{50} DS 0982 isolate, β-1,6 glucan biosynthesis protein-like protein was also upregulated. β-1,6 glucan biosynthesis will likely result in a greater abundance of cross-linkages within the cell wall thus increasing its rigidity. This β-1,6 glucan biosynthesis protein-like protein upregulation in DS 0982 was in stark contrast with the lack of a similar response in low-ED_{50} isolate DS 1091. Corroborating these findings, another protein identified as the cell wall assembly and cell proliferation coordinating protein (SMI1) was also differentially regulated in the two isolates in response to NaCl stress (Fig. 4). In sum, while the fast-growing, low-ED_{50} isolate DS 1091 may have reduced cell wall synthesis and maintenance of its rigidity in response to NaCl stress, the slow-growing, high-ED_{50} isolate DS 0982 responded by upregulating proteins responsible for cell wall synthesis and cell wall modification, such as SMI1, likely resulting in adjustments in structural strategy and subsequent cell wall strengthening.

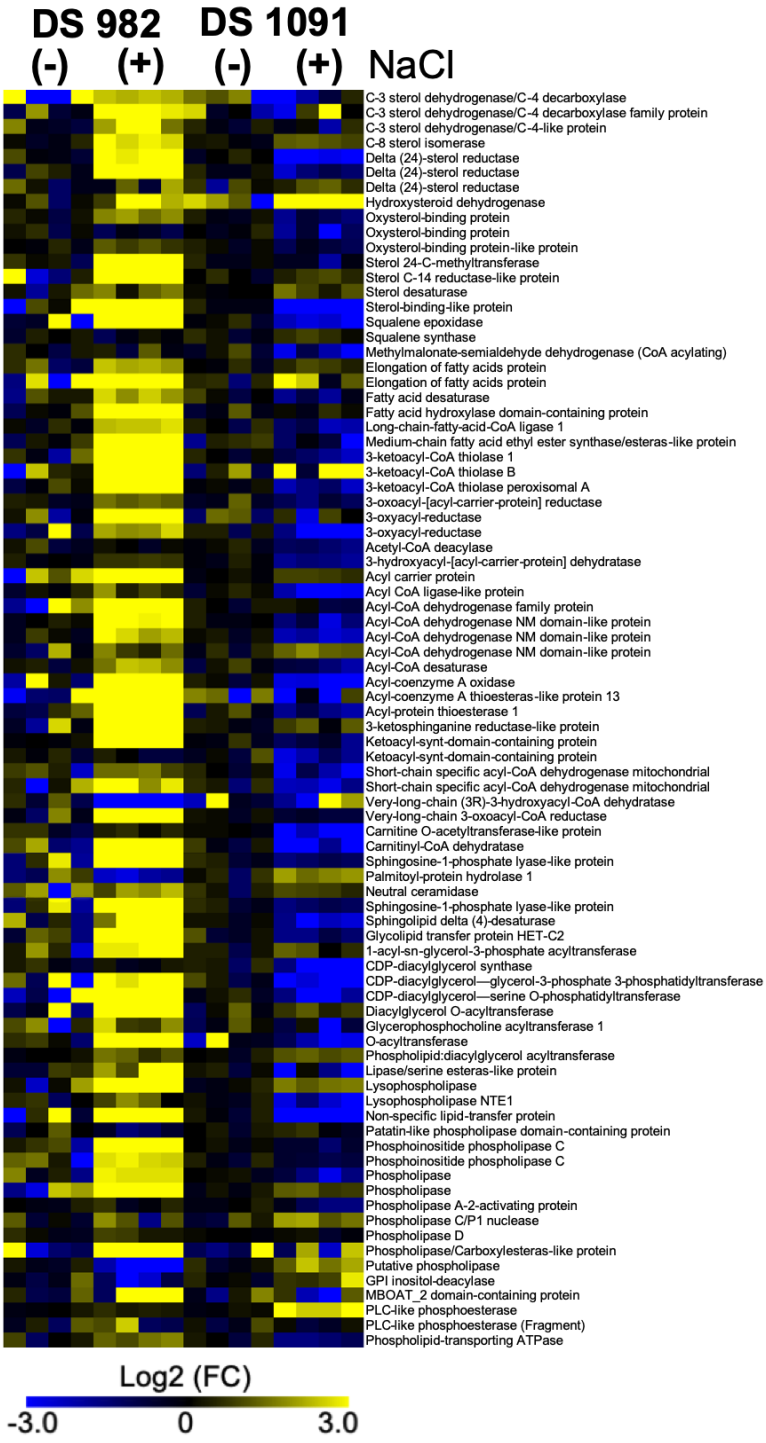

Figure 5. Cell Membrane Proteomic Response of *P. macrospinosa* to NaCl. Relevant membrane protein abundances are listed in the heatmap and separated by isolate and condition. A complete list of select relevant lipid proteins and their abundances is available in the supplemental Table S6.

Cell Membrane Lipid-Associated Proteomic Responses in *P. macrospinosa*

We observed a variety of *P. macrospinosa* membrane lipid responses to salinity (Fig. 5). We used MEV software to visualize salinity-affected membrane lipid proteins that were selected based on keyword searches. In the slow-growing DS 0982 isolate, the cell membrane associated protein abundances tended to increase in response to salt stress. In contrast, in the fast-growing isolate DS 1091, those proteins tended to decrease in relative abundance. These data support the strong, relative positive response in the slow-growing, high ED_{50} isolate and an opposite response in the fast-growing, low ED_{50} isolate.

The cell membrane is the final barrier that separates the cell cytosol from the external environment. The cell membranes are essential in halostress tolerance as they regulate cellular responses and defenses in response to the extracellular environment (Hohmann 2002). In general, membrane exposure to hyper-saline stress implies inherent hyperosmotic impacts such as passive membrane-permeating water efflux or dehydration (Lerici et al. 1988; Raoult-Wack et al. 1992; Guilbert 1994; Raoult-Wack 1994; Rahman MS and Labuza 1999; Tortoe 2010; Yadav and Singh 2014), loss of turgor pressure (Hohmann 1997; Mager and Siderius 2002), increase in internal solute concentrations (Yancey et al. 1982; Mager and Varela 1993; Jin et al. 2005), challenges of osmotic and ionic stress (Hohmann 2002; Szopinska et al. 2011), osmotically induced oxidative stress (Moran et al. 1994; Serrano et al. 1999), turgor-mediated growth suppression (Kempf and Bremer 1998; Blomberg 2000), expected ion-mediated metabolic inhibition (Murguía et al. 1995; 1996), general aversion to enzymatic activity (Wyn Jones and Pollard 1983), and imbalance in the membrane potential (Norbeck and Blomberg 1998).

Turgor pressure is necessary for cell survival and growth (Blomberg 1997). Thus, it is critical that cells in the fungal hyphae regulate cytoplasmic volume during hyphal growth under

desiccating conditions. During hyphal growth, cytoplasmic streaming occurs throughout the hyphal network and is regulated by cytoplasmic turgor pressure and microtubule-based motors (Steinberg 2007). The microtubule motors transport vesicles as well as resources and cell wall materials necessary for hyphal tip elongation, cell division, hyphal septation, and cytoplasmic expansion against newly developed cell walls (Geitmann and Emons 2000). During this cell wall material delivery, the growth site at the hyphal tip – the Spitzenkörper (Roberson 2020) – aid in the exoenzyme secretion (Harris et al. 2005) by means of an induced isotropic pressure gradient (Bartnicki-Garcia 2002). These exoenzymes break down extracellular substrates for colony use and are involved in synthesizing new, elastic, and non-rigid cell walls (Archer and Wood 1995; Gooday 1995; Chao et al. 2014; Xie and Miao 2021) necessary for hyphal shaping and elongation through turgor-driven cytoplasmic expansion (Sietsma and Wessels 1994).

The cellular membrane is water permeable. When challenged with external compatible solutes or osmolytes, such as NaCl ions (Yancey 2005), it regulates the intracellular tonicity or effective osmolarity. During osmotic challenge, the extracellular osmotic agents create a hyperosmotic gradient that effectively draws ions into the cell and water from the cytosol through a process known as osmotic dehydration (Serrano et al. 1999; Tortoe 2010; Yadav and Singh 2014). Cellular desiccation and loss of intracellular water can be detrimental to the cell and negatively affects the intracellular water activity. Low water activity, or the low reactive potential of free water, limits fungal growth (Rahman and Labuza 1999) by decreasing the cytosolic volume and turgor pressure, diminishing potential cytoplasmic streaming, and restricting hyphal tip extension, as well as concentrating potentially harmful osmolytes within the cytoplasm (Rahman and Labuza 1999; Tortoe 2010).

The fungal cell membrane consists of a phospholipid bilayer (Wang et al. 2019) entrenched with transmembrane proteins involved in cell wall biosynthesis, active transport against gradients, and signal transduction (Douglas and Konopka 2016). The protein activity within the plasma membrane has even been reported to affect regulation of cell polarity and growth (Los and Murata 2004). Lipids are critical to membrane structure, function, composition, and permeability and belong to three major classes: glycerophospholipids, sphingolipids and sterols (Sant et al. 2016).

Glycerophospholipids are the structural backbone lipids of plasma membranes and facilitate their proper fluidity and ion permeability (Farooqui 2014). Sphingolipids are key components of cell membranes, especially in filamentous fungi, where they are essential for polarisome organization at the hyphal tip (Fontaine 2017). Polarisomes assist to direct the cell polarity and mediate actin remodeling for cell segregation (Liu et al. 2010) and transport (Xie and Miao 2021). Some even suggest that filamentous growth and hyphal formation may be entirely dependent on polarisome action (Xie et al. 2020) through actin cable polarization (Steinberg 2007), and the subsequent potential to direct the Spitzenkörper to the hyphal filament apex – directing this hyphal tip elongation (Crampin et al. 2005). Glycerophospholipids and sphingolipids are collectively involved in cell function and signal transduction pathways (Sant et al. 2016) as well as DNA replication and cell trafficking (Dowhan 1997; Doufourc 2008).

Sphingolipids, aside from membrane structure contributions, also likely play several roles in cell function. Sphingolipid biosynthesis requires the precursor starting materials known as very long chain fatty acids (Nie et al 2021). The elongation of fatty acids to develop these essential sphingolipid building blocks is facilitated by specialized proteins. Both very-long-chain 3-oxoacyl-CoA reductase and elongation of fatty acid proteins were upregulated in the slow-

growing, high-ED_{50} isolate DS 0982 and changed inconsistently in the fast-growing, low-ED_{50} isolate DS 1091 in response to osmostress indicating differences in their membrane modifications (Fig. 5). Both of these proteins have been suggested to be involved in the development of very-long-chain fatty acids used in sphingolipid synthesis (Beaudoin et al. 2002; Han et al. 2002; Beaudoin et al. 2009) and therefore central to plasma membrane structuring.

Consistent with the responses of the slow-growing DS 0982, sphingolipid production has been suggested to improve osmotic tolerance in fungi (Zhu et al 2020). Further, protein facilitated transport at the fungal membrane requires ATPases for energy transfer, particularly for cellular excretion; sphingolipid synthesis has been reported as a requirement for ATPase routing toward the cell membrane (Gaigg et al. 2005), potentially promoting additional osmoregulatory efforts. Sphingolipids also act with sterols to create structural and functional lipid rafts in fungal membranes that are involved in protein organization and sorting, cell polarity, and secretion (Bagnat and Simons 2002; Wachtler and Balasubramanian 2006; Alvarez et al. 2007).

Sterols, especially the most abundant ergosterol (Rodrigues 2018), are possibly the most important lipids in the fungal membrane (Zinser et al. 1991). These sterols are likely effective structural membrane reinforcement (Ribeiro et al. 2007) and regulate membrane fluidity and permeability (Douglas and Konopka 2014; Rodrigues 2018) as well as ion homeostasis (Li et al. 2021). Sterol biosynthesis, particularly that of membrane ergosterol, is critical to membrane success and response (Dhingra and Cramer 2017).

The abundance profiles listed in Fig. 5 demonstrate several interesting protein responses to salinity within our isolates. First, CDP-diacylglycerol synthase is upregulated in the slow-growing, high-ED_{50} isolate DS 0982 in response to salt. CDP-diacylglycerol synthase is an initial

enzyme in sterol biosynthesis and produces CDP-diacylglycerol, a key lipid precursor (Carman and Han 2011). Second, we observed a correlated response of sterol C-14 reductase-like protein, that is reportedly crucial to membrane integrity as a regulator of both ergosterol biosynthesis and ion homeostasis (Li et al. 2021). Further support for increased sterol biosynthesis is highlighted in the response of sterol 24-C methyltransferase, the last enzymatic step in sterol biosynthesis (Zinser et al. 1993). Hyperosmotic conditions, created by the external NaCl ion challenge, have been suggested to reduce membrane fluidity, to correlate with ion permeability, and increase membrane rigidity, likely through the addition of membrane sterols – resulting in an increased membrane sterol composition (Los and Murata 2004). In contrast to the high-ED_{50} isolate DS 0982, the low-ED_{50} isolate DS 1091 expressed a decreased abundance in these proteins, suggesting a relative downregulation in sterol biosynthesis likely to lead to decreased rigidity and increased permeability.

References

Adams D. 2004. Fungal cell wall chitinases and glucanases. Microbiology. 150(7):2029-2035.

Alvarez FJ, Douglas LM, Konopka JB. 2007. Sterol-rich plasma membrane domains in fungi. Eukaryot Cell. 6(5):755-763.

Archer DB and Wood DA. 1995. Fungal exoenzymes. In: Gow NAR and Gadd GM, eds. The growing fungus. Chapman and Hall, London, United Kingdom: 135-162.

Babazadeh R, Furukawa T, Hohmann S, Furukawa K. 2014. Rewiring yeast osmostress signalling through the MAPK network reveals essential and non-essential roles of Hog1 in osmoadaptation. Sci. Rep. 4:4697.

Bagnat M and Simons K. 2002. Lipid rafts in protein sorting and cell polarity in budding yeast Saccharomyces cerevisiae. Biol Chem. 383(10):1475-1480.

Bahn YS, Xue C, Idnurm A, Rutherford JC, Heitman J, Cardenas ME. 2007. Sensing the environment: lessons from fungi. Nat Rev Microbiol. 5:57-69.

Bartnicki-Garcia S, Bracker CE, Gierz G, López-Franco R, Lu H. 2000. Mapping the growth of fungal hyphae: orthogonal cell wall expansion during tip growth and the role of turgor. Biophys J. 79(5):2382-2390.

Bartnicki-Garcia S. 2002. Molecular biology of fungal development. Marcel Dekker, New York, NY:29-58.

Beaudoin F, Gable K, Sayanova O, Dunn T, Napier JA. 2002. A Saccharomyces cerevisiae gene required for heterologous fatty acid elongase activity encodes a microsomal beta-keto-reductase. The Journal of Biological Chemistry. 277(13):11481–11488.

Beaudoin F, Wu X, Li F, Haslam RP, Markham JE, Zheng H, Napier JA, Kunst L. 2009. Functional characterization of the Arabidopsis beta-ketoacyl-coenzyme A reductase candidates of the fatty acid elongase. Plant Physiology. 150(3):1174–1191.

Blomberg A and Adler L. 1992. Physiology of osmotolerance in fungi. Adv. Microb. Phys. 33:145–212.

Blomberg A. 1997. The osmotic hypersensitivity of the yeast Saccharomyces cerevisiae is strain and growth media dependent: quantitative aspects of the phenomenon. Yeast. 13:529–539.

Blomberg A. 2000. Metabolic surprises in Saccharomyces cerevisiae during adaptation to saline conditions: questions, some answers and a model. FEMS Microbiology Letters. 182(1):1–8.

Bowman SM and Free SJ. 2006. The structure and synthesis of the fungal cell wall. Bioessays. 28(8):799-808.

Carman GM and Han GS. 2011. Regulation of phospholipid synthesis in the yeast Saccharomyces cerevisiae. Annu Rev Biochem. 80:859-883.

Carman, G.M. and Han, G.-S. (2011) Regulation of phospholipid synthesis in the yeast Saccharomyces cerevisiae. Antimicrob Agents Chemother 80, 859–883.

Chao JT, Wong AKO, Tavassoli S, Young BP, Chruscicki A, Fang NN, Howe LAJ, Mayor T, Foster LJ, Loewen CJR. 2014. Polarization of the endoplasmic reticulum by ER-septin tethering. Cell. 158:620-632.

Dhingra S and Cramer RA. 2017. Regulation of Sterol Biosynthesis in the Human Fungal Pathogen Aspergillus fumigatus: Opportunities for Therapeutic Development. Front Microbiol. 8:92.

Douglas LM and Konopka JB. 2014. Fungal membrane organization: the eisosome concept. Annu Rev Microbiol. 68:377-393.

Dowhan W. 1997. Molecular basis for membrane phospholipid diversity: why are there so many lipids?. Annu Rev Biochem. 66:199-232.

Dufourc EJ. 2008. Sterols and membrane dynamics. J Chem Biol. 1(4):63-77.

Ene IV, Walker LA, Schiavone M, Lee KK, Martin-Yken H, Dague E, Gow NA, Munro CA, Brown AJ. 2015. Cell Wall Remodeling Enzymes Modulate Fungal Cell Wall Elasticity and Osmotic Stress Resistance. mBio. 6(4):e00986.

Farooqui AA. 2014. Glycerophospholipids. In: eLS, John Wiley & Sons, Ltd (Ed.).

Fesel PH and Zuccaro A. 2016. β-glucan: Crucial component of the fungal cell wall and elusive MAMP in plants. Fungal Genet Biol. 90:53-60.

Fontaine T. 2017. Sphingolipids from the human fungal pathogen Aspergillus fumigatus. Biochimie. 141:9–15.

Free SJ. 2013. Fungal cell wall organization and biosynthesis. Adv. Genet. 81:33–82.

Gaigg B, Timischl B, Corbino L, Schneiter R. 2005. Synthesis of sphingolipids with very long chain fatty acids but not ergosterol is required for routing of newly synthesized plasma membrane ATPase to the cell surface of yeast. J Biol Chem. 280(23):22515-22522.

Garcia-Rubio R, de Oliveira HC, Rivera J, Trevijano-Contador N. 2020. The Fungal Cell Wall: Candida, Cryptococcus, and Aspergillus Species. Front. Microbiol. 10:2993.

Geitmann A and Emons AM. 2000. The cytoskeleton in plant and fungal cell tip growth.

Gooday GW. 1995. Cell walls. In: Gow NAR and Gadd GM, eds. The growing fungus. Chapman and Hall, London, United Kingdom:41-62.

Gostinčar C, Lenassi M, Gunde-Cimerman N, Plemenitaš A. 2011. Fungal Adaptation to Extremely High Salt Concentrations. Advances in Applied Microbiology. 3(77):71-96.

Gow NAR, Latge JP, Munro CA. 2017. The Fungal Cell Wall: Structure, Biosynthesis, and Function. Microbiol Spectr. 2017 May;5(3).

Guilbert S. 1994. Edible coatings and osmotic dehydration, Food Preservation by Combined Processes. In: Leistner L and Gorris LGM, eds. FLAIR Final Report, EUR 15776 EN, European Commission, Brussels. 1994:65.

Hagiwara D, Yoshimi A, Sakamoto K, Gomi K, Abe K. Response and adaptation to cell wall stress and osmotic stress in Aspergillus species. Stress Biology of Yeasts and Fungi. Tokyo: Springer Japan. 2015:199–218.

Han G, Gable K, Kohlwein SD, Beaudoin F, Napier JA, Dunn TM. 2002. The Saccharomyces cerevisiae YBR159w gene encodes the 3-ketoreductase of the microsomal fatty acid elongase. The Journal of Biological Chemistry. 277(38):35440–35449.

Harris SD, Read ND, Roberson RW, Shaw B, Seiler S, Plamann M, Momany M. 2005. Polarisome meets spitzenkörper: microscopy, genetics, and genomics converge. Eukaryot Cell. 4(2):225-229.

Hartland RP, Vermeulen CA, Klis FM, Sietsma JH, Wessels JG. 1994. The linkage of (1-3)-beta-glucan to chitin during cell wall assembly in Saccharomyces cerevisiae. Yeast. 10(12):1591-1599.

Hohmann S and Mager WH. 1997. Shaping up: the response of yeast to osmotic stress. In: Hohmann S, Mager WH, eds. Yeast stress responses. R. G. Landes Company, Austin, Tex. 1997:101-145.

Hohmann S. 2002. Osmotic adaptation in yeast--control of the yeast osmolyte system. Int Rev Cytol. 215:149-187.

Hopke A, Brown AJP, Hall RA, Wheeler RT. 2018. Dynamic Fungal Cell Wall Architecture in Stress Adaptation and Immune Evasion. Trends Microbiol. 26(4):284-295.

J Microsc. 198(3):218-245.

Jin Y, Weining S, Nevo E. 2005. A MAPK gene from Dead Sea fungus confers stress tolerance to lithium salt and freezing-thawing: Prospects for saline agriculture. Proc Natl Acad Sci. 102(52):18992-18997.

Kempf B and Bremer E. 1998. Uptake and synthesis of compatible solutes as microbial stress responses to high-osmolality environments. Arch Microbiol. 170:319–330.

Klein M, Swinnen S, Thevelein JM, Nevoigt E. 2016. Glycerol metabolism and transport in yeast and fungi: established knowledge and ambiguities. Environmental Microbiology. 19(3):878-893.

Klis FM, De Groot P, Hellingwerf K. 2001. Molecular organization of the cell wall of Candida albicans. Medical Mycology. 39(1):1-8.

Kollár R, Petráková E, Ashwell G, Robbins PW, Cabib E. 1995. Architecture of the yeast cell wall. The linkage between chitin and beta(1-->3)-glucan. J Biol Chem. 270(3):1170-1178.

Kollár R, Reinhold BB, Petráková E, Yeh HJ, Ashwell G, Drgonová J, Kapteyn JC, Klis FM, Cabib E. 1997. Architecture of the yeast cell wall. Beta(1-->6)-glucan interconnects mannoprotein, beta(1-->)3-glucan, and chitin. J Biol Chem. 272(28):17762-17775.

Latgé JP. 2007. The cell wall: a carbohydrate armour for the fungal cell. Molecular Microbiology. 66(2):279-290.

Lerici CR, Mastrocola D, Sensidoni A, Dalla Rosa M. 1988. Osmotic concentration in food processing. In: Preconcentration and Drying of Food Materials, Bruin S, ed. Elsevier Applied Science Publishers, Amsterdam. 1988:123.

Li M, Jiang C, Wang Q, Zhao Z, Jin Q, Xu JR, Liu H. 2016. Evolution and Functional Insights of Different Ancestral Orthologous Clades of Chitin Synthase Genes in the Fungal Tree of Life. Front Plant Sci. 7:37.

Li Y, Dai M, Zhang Y, Lu L. 2021. The sterol C-14 reductase Erg24 is responsible for ergosterol biosynthesis and ion homeostasis in Aspergillus fumigatus. Appl Microbiol Biotechnol. 105(3):1253-1268.

Liu B, Larsson L, Caballero A, Hao X, Oling D, Grantham J, Nyström T. 2010. The polarisome is required for segregation and retrograde transport of protein aggregates. Cell. 140(2):257-267.

Los DA and Murata N. 2004. Membrane fluidity and its roles in the perception of environmental signals. Biochim Biophys Acta. 1666(2):142-157.

Mager WH and Siderius M. 2002. Novel insights into the osmotic stress response of yeast. FEMS Yeast Res. 2(3):251-257.

Mager WH and Varela JC. 1993. Osmostress response of the yeast *Saccharomyces*. Mol Microbiol. 10(2):253-258.

Mouyna I, Morelle W, Vai M, Monod M, Léchenne B, Fontaine T, Beauvais A, Sarfati J, Prévost MC, Henry C, Latgé, JP. 2005. Deletion of GEL2 encoding for a β(1–3)glucanosyltransferase affects morphogenesis and virulence in Aspergillus fumigatus. Molecular Microbiology. 56:1675-1688.

Munro CA, Winter K, Buchan A, Henry K, Becker JM, Brown AJ, Bulawa CE, Gow NA. 2001. Chs1 of Candida albicans is an essential chitin synthase required for synthesis of the septum and for cell integrity. Mol Microbiol. 39(5):1414-1426.

Murguía JR, Bellés JM, Serrano R. 1995. A salt-sensitive 3'(2'),5'-bisphosphate nucleotidase involved in sulfate activation. Science. 267(5195):232-234.

Murguía JR, Bellés JM, Serrano R. 1996. The yeast HAL2 nucleotidase is an in vivo target of salt toxicity. J Biol Chem. 271(46):29029-29033.

Muszewska A, Piłsyk S, Perlińska-Lenart U, Kruszewska JS. 2018. Diversity of Cell Wall Related Proteins in Human Pathogenic Fungi. J Fungi (Basel). 4(1):6.

Nie L, Pascoa TC, Pike ACW, Bushell SR, Quigley A, Ruda GF, Chu A, Cole V, Speedman D, Moreira T, Shrestha L, Mukhopadhyay SMM, Burgess-Brown NA, Love JD, Brennan PE, Carpenter EP. 2021. The structural basis of fatty acid elongation by the ELOVL elongases. Nat Struct Mol Biol. 28(6):512-520.

Norbeck J and Blomberg A. 1998. Amino acid uptake is strongly affected during exponential growth of *Saccharomyces cerevisiae* in 0.7 M NaCl medium. FEMS Microbiol Lett. 158(1):121-126.

Okada N, Tatsuno L, Hanski E, Caparon M, Sasakawa C. 1998. A 1,3-beta-glucanosyltransferase isolated from the cell wall of Aspergillus fumigatus is a homologue of the yeast Bgl2p. Microbiology. 144(11):3079-3086.

Pascual-Ahuir A, Manzanares-Estreder S, Timón-Gómez A, Proft M. 2018. Ask yeast how to burn your fats: lessons learned from the metabolic adaptation to salt stress. Curr Genet. 64:63–69 (2018).

Rahman MS and Labuza TP. 1999. Water activity and food preservation. In: Handbook of food preservation, Rahman MS ed. Marcel Dekker, New York. 1999:339–382.

Raoult-Wack AL, Guilbert S, Lenart A. 1992. Recent advances in drying through immersion in concentrated solutions, Drying of Solids. In: Mujumdar AS, ed. International Science Publishers, New York. 1992:21.

Raoult-Wack AL. 1994. Recent advances in the osmotic dehydration of foods. Trends Food Sci Technol. 5:255.

Ribeiro N, Streiff S, Heissler D, Elhabiri M, Albrecht-Gary AM, Atsumi M, Gotoh M, Desaubry L, Nakatani Y, Ourisson G. 2007. Reinforcing effect of bi- and tri-cyclopolyprenols on ‘primitive’ membranes made of polyprenyl phosphates. Tetrahedron. 63:3395–3407.

Roberson R. 2020. Subcellular structure and behaviour in fungal hyphae. Journal of Microscopy. 280:75-85.

Rodrigues ML. 2018. The Multifunctional Fungal Ergosterol. mBio. 9(5):e01755-18.

Román E, Correia I, Prieto D, Alonso R, and Pla, J. 2020. The HOG MAPK pathway in Candida albicans: more than an osmosensing pathway. International Microbiology 23(1):23-29.

Roncero C, Vázquez de Aldana CR. 2020. Glucanases and Chitinases. Curr Top Microbiol Immunol. 425:131-166.

Sant D, Tupe S, Ramana C, Deshpande M. 2016. Fungal cell membrane—promising drug target for antifungal therapy. J Appl Microbiol. 121:1498-1510.

Serrano R, Mulet JM, Rios G, Marquez JA, de Larrinoa IF, Leube MP, Mendizabal I, Pascual-Ahuir A, Proft M, Ros R, Montesinos C. 1999. A glimpse of the mechanisms of ion homeostasis during salt stress. Journal of Experimental Botany. 50:1023–1036.

Shaw JA, Mol PC, Bowers B, Silverman SJ, Valdivieso MH, Durán A, Cabib E. 1991. The function of chitin synthases 2 and 3 in the Saccharomyces cerevisiae cell cycle. J Cell Biol. 114(1):111-123.

Sietsma J and Wessels J. 1994. Apical wall biogenesis. In: Wessels J and Meinhardt F, eds. The Mycota. Springer-Verlag, Berlin, Germany. 1:126-141

Steinberg G. 2007. Hyphal growth: a tale of motors, lipids, and the Spitzenkörper. Eukaryot Cell. 6(3):351-360.

Szopinska A, Degand H, Hochstenbach JF, Nader J, Morsomme P. 2011. Rapid response of the yeast plasma membrane proteome to salt stress. Mol. Cell. Proteom. 10:M111.009589.

Takaya N, Yamazaki D, Horiuchi H, Ohta A, Takagi M. 1998. Cloning and characterization of a chitinase-encoding gene (chiA) from Aspergillus nidulans, disruption of which decreases germination frequency and hyphal growth. Biosci Biotechnol Biochem. 62:60–65

Tortoe C. 2010. A review of osmodehydration for food industry. African Journal of Food Science. 4(6):303-324.

Wachtler V and Balasubramanian MK. 2006. Yeast lipid rafts?--an emerging view. Trends Cell Biol. 16(1):1-4.

Wang J, Wang H, Zhang C, Wu T, Ma C, Chen Y. 2019. Phospholipid homeostasis plays an important role in fungal development, fungicide resistance and virulence in Fusarium graminearum. Phytopathol Res. 1:16.

Wyn Jones RG and Pollard A. 1983. Proteins, enzymes and inorganic ions. In: Lau¨chli A, Pirson A, eds. Encyclopedia of Plant Physiology. 15(B):528–562.

Xie Y, Loh ZY, Xue J, Zhou F, Sun J, Qiao Z, Jin S, Deng Y, Li H, Wang Y, Lu L, Gao Y, Miao Y. 2020. Orchestrated actin nucleation by the Candida albicans polarisome complex enables filamentous growth. J. Biol. Chem. 29:14840-14854.

Xie Yand Miao Y. 2021. Polarisome assembly mediates actin remodeling during polarized yeast and fungal growth. J Cell Sci. 134(1):jcs247916.

Yadav AK and Singh SV. 2014. Osmotic dehydration of fruits and vegetables: a review. J Food Sci Technol. 51(9):1654-1673.

Yancey PH, Clark ME, Hand SC, Bowlus RD, Somero GN. 1982. Living with water stress: evolution of osmolyte systems. Science. 217(4566):1214-2122.

Zhu G, Yin N, Luo Q, Liu J, Chen X, Liu L, Wu J. 2020. Enhancement of Sphingolipid Synthesis Improves Osmotic Tolerance of Saccharomyces cerevisiae Applied and Environmental Microbiology. 86(8):e02911-19.

Zinser E, Paltauf F, Daum G. 1993. Sterol composition of yeast organelle membranes and subcellular distribution of enzymes involved in sterol metabolism. J Bacteriol. (10):2853-2858.

Zinser E, Sperka-Gottlieb CD, Fasch EV, Kohlwein SD, Paltauf F, Daum G. 1991. Phospholipid synthesis and lipid composition of subcellular membranes in the unicellular eukaryote Saccharomyces cerevisiae. J Bacteriol. 173(6):2026-2034.

5. Results & Discussion: Evidence and Impacts of the High-Osmolarity Glycerol Pathway

The KEGG pathway enrichment analysis strongly indicated that the MAPK signaling pathway was upregulated in the slow-growing, high-ED_{50} isolate DS 0982 (Fig. 3) in response to salt. The response was opposite in the fast-growing, low-ED_{50} isolate DS 1091, whose MAPK signaling pathway was downregulated in response to salt stress. This inverse response of such a critical pathway may provide insight into the overall functions and interactive mechanisms of our two isolates' salt tolerance strategies and their use of the High-Osmolarity Glycerol (HOG) pathway. The HOG pathway responds to changes in osmotic pressure that correlate with changes in intracellular volume as a result of a salinity challenge (Duran et al. 2010). The salt challenge chosen for our study corroborates prior reports that a salinity challenge of 0.4 M NaCl causes a prompt 20% loss of cell volume and effectively results in Hog1 nuclear transport (Babazadeh et al. 2014; Stojanovski et al 2017; Tatebayashi et al. 2020). Our data indicated an array of differential responses among the two *P. macrospinosa* isolates ranging from compatible osmolyte production to transcriptional regulation and changes in cell cycle regulation. To validate these results and correlate them with their relative upstream and downstream effects, we mapped our proteome data to the HOG pathway (Fig. 6).

Past research has characterized MAPK signaling proteins present in *Saccharomyces cerevisiae* and identified fungal homologues across taxa and lifestyles (Martínez-Soto and Ruiz-Herrera 2017). The HOG pathway is a MAPK signaling pathway subcomponent and highly conserved across all fungi (Bansal et al. 2001; El-Mowafy et al. 2013; Konte et al. 2016). Further, *S. cerevisiae* HOG pathway systems have previously been used as models for orthologous signaling proteins (Konte et al. 2016). Seventeen of the twenty-one detected proteins

annotated to *S. cerevisiae* homologues and associated with the complex HOG histidine-kinase cascade demonstrated significant differences in abundance across the isolates and conditions. The HOG pathway is a highly conserved, interconnected, and multifaceted series of cascades and protein interactions which operate as adaptive response regulators such as the linchpin MAPK: Hog1 (Konte et al. 2016).

Current understanding of the upstream membrane-bound sensory proteins directly interacting with the HOG pathway suggests a bifurcated regulation, in which two major contributing osmosensory proteins are required for initial stimulus response – Sln1 and Sho1 (Hohmann 2015). While both pathways offer relative regulatory redundancy, they do so in distinctly unique ways. The Sln1 branch utilizes a multi-step inhibitive activation osmodetection cascade, whereas the Sho1 branch has direct osmodetection to multi-step, multi-channel cascades that utilize phosphorylative complexes. The Sln1-activated branch operates as a two-component signal transduction system (TCS) and involves the membrane-bound osmosensor Sln1, the intermediary phosphorelay protein Ypd1, and the cytoplasmic response regulative protein Ssk1 (Posas et al. 1996). At low to normal extracellular osmolarities the Sln1 osmosensor is activated via phosphorylation and inhibits Ypd1 mediation, ultimately resulting in the phosphorylation of Ssk1 and the subsequent inhibition of the TCS Sln1-Ypd1-Ssk1 phosphorelay (Dexter et al. 2015). High extracellular osmolarity results in the Sln1 inactivation, allowing the targeted MAPK Ssk2-Pbs2-Hog1 phosphorelay activation resulting from the dephosphorylation of the Ssk1 cascade regulator (Posas et al. 1996; Posas and Saito 1998).

In both *P. macrospinosa* isolates included in this study, the osmosensor Sln1 abundance declined in response to salt, suggesting a subsequent HOG pathway upregulation. However, the intermediary phosphorelay protein Ypd1 was also heavily upregulated in response to salinity in

our slow-growing, high-ED_{50} DS 0982 isolate, but not in our fast-growing, low-ED_{50} DS 1091 isolate, indicating a stronger TCS Sln1 branch response in DS 0982 than that observed in DS 1091. During Ssk2-Pbs2-Hog1 cascade activation, Ssk1 – unphosphorylated via Ypd1 of the TCS phosphorelay – interacts with the MAP kinase kinase kinase (MAPKKK) protein Ssk2. While Ssk2 seems to have been upregulated in response to salinity in DS 0982, the comparisons both within and across isolates in response to salt indicated no significant differences. MAPKKK Ssk2 proteins continue the cascade response activating the MAP kinase kinase (MAPKK) Pbs2, which directly regulates the MAPK Hog1. In the high-ED_{50} DS 0982 isolate, Pbs2 protein abundance was upregulated in response to salinity, whereas, in contrast, it was downregulated in the low-ED_{50} DS 1091 isolate (Fig. 6). Because of the sequential activation of Pbs2 to Hog1, especially during osmotic stress (Tatebayashi et al. 2020), the DS 0982 isolate likely upregulated Hog1 activation, whereas the fast-growing, low- ED_{50} DS 1091 isolate likely downregulated it.

In contrast to Sln1 osmosensor that was upregulated in both of our *P. macrospinosa* isolates, the Sho1 osmosensor was upregulated in the slow-growing, high-ED_{50} DS 0982 isolate but was downregulated in the fast-growing DS 1091 isolate. The Sho1 osmoadaptive branch utilizes the membrane anchored Sho1 protein, which interacts with associated osmosensory proteins to initiate a response to high osmolarity (Fettich et al. 2011). The Sho1 branch activates the downstream MAPKKK Ste11 and does so through an intricate set of interactions between several upstream response regulative proteins (Posas and Saito 1997). Sho1 abundances were highly upregulated in DS 0982 in response to salinity and downregulated in DS 1091. This response in Sho1 osmosensor abundance indicates an increased investment in Sho1 branch osmosensing efforts and a resultant overall increase in HOG pathway activation and subsequent osmoadaptive efforts in DS 0982 in response to prolonged salinity. Inversely, DS 1091 is

demonstrating a disinvestment in the Sho1 branch and an implied resultant decrease in overall HOG pathway activation and osmoadaptive response. The activated Sho1 phosphorylates the guanosine-triphosphatase (GTPase) Cdc42 and recruits Cdc24, a guanine nucleotide exchange factor (GEF) for their co-involvement in the activation of the MAP kinase kinase kinase kinase (MAPKKKK) Ste20 (Raitt et al. 2000). This disinvestment of DS 1091 into the Sho1 branch may implicate serious consequences due to a lack of sensitivity of the HOG pathway as a result of downregulation of Sho1 osmosensing and the effective regulatory and adaptive responses that will be unable to phosphorelay downstream due to the decreased Sho1 activity. DS 0982 on the other hand evidently is investing in upregulation of Sho1 which may provide not only a higher osmosensitivity but result in greater HOG pathway regulatory and adaptive activity due to Sho1 interaction and downstream phosphorelay interactions.

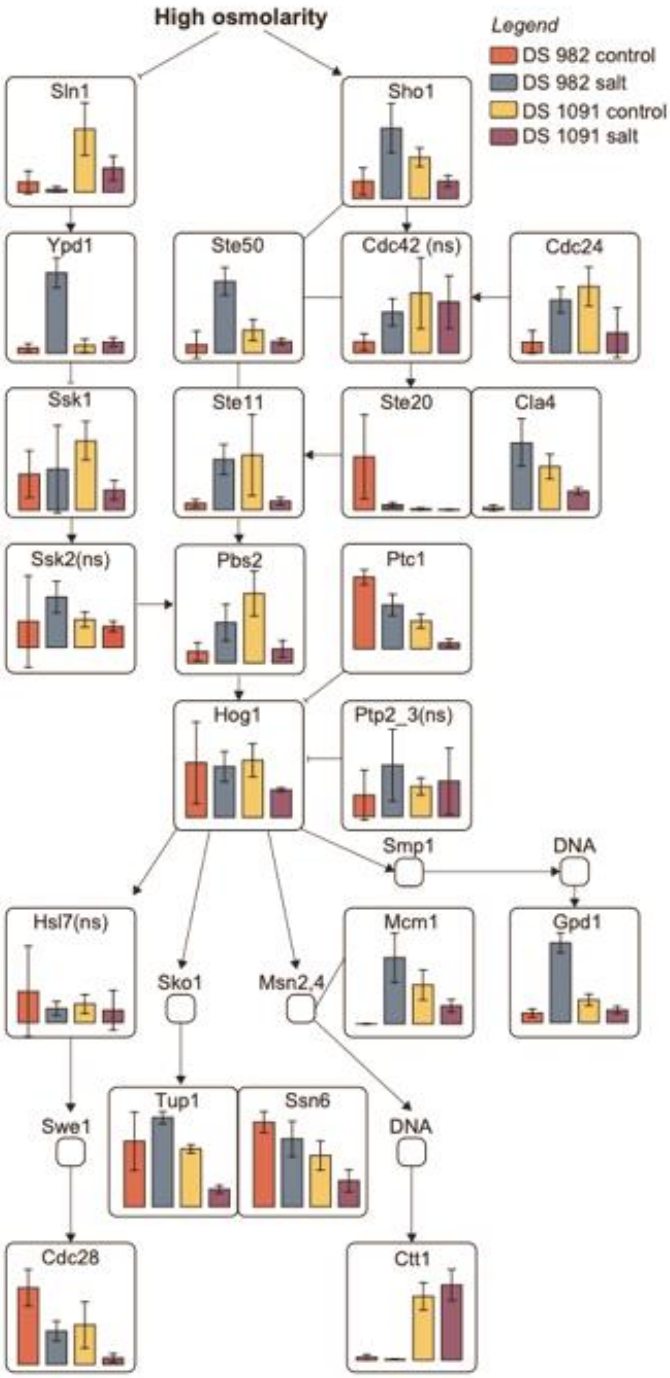

Figure 6. High Osmolarity Glycerol (HOG) Pathway Response of *P. macrospinosa* to NaCl stress. The figure shows the relative abundance of proteins involved in the HOG pathway in the slow-growing, high-ED_{50} DS 0982 and fast-growing, low-ED_{50} DS 1091 *P. macrospinosa* isolates. Proteins followed by (ns) did not differ in any of the four comparisons (*t*-test; $P \geq 0.05$). Complete comparisons between the different samples and abundances of each analyte are shown in the supplemental Table S5.

As Sho1 activates Cdc42, which recruits Cdc24 for a coupled interaction with Ste20 for downstream activation of the keystone HOG1 protein, a second Ste20 initiator also plays a part in co-regulating this downstream activation. The HOG pathway recruits Cla4, a protein redundant with GEF-Cdc24, to assist in activating the MAPKKKK protein Ste20 (Tatebayashi et al. 2006). Both Cdc24 and Cla4 were upregulated in DS 0982 and downregulated in DS 1091 further confirming the distinct and opposite HOG pathway responses in the two *P. macrospinosa* isolates. Activation of Ste20 by the coupled interactions of the GEF Cdc42 and GTPase-like proteins Cdc24/Cla4, which together form the Cdc42-Ste20 complex, is facilitated by the scaffolding interaction with the membrane anchor associate Ste50. Ste50 binds to another, membrane-anchored Ste11 protein to form a Ste50-Ste11 complex – an integral requirement for Sho1-Ste11 activation of the HOG pathway (Posas and Saito 1998).

It is also understood that Ste50 is involved in regulating mating signaling and filamentous growth response in fungi (Ramezani-Rad 1998). Ste50 abundances in response to salt increased in DS 0982 and correlated with and supported our observations of high ED_{50} and maintenance of the observed continuous growth under salt stress, whereas DS 1091 showed little to no Ste50 response to salinity. Ste50 acts as an adapter that facilitates connection between the Cdc42-Ste20 complex and Ste11 (Ramezani-Rad 2003). The Ste11-Ste50 complex subsequently binds with the Cdc42-Ste20 complex that facilitates activation of Cdc24/Cla4 to act on Ste20 and also provides the activated proteins to Ste11.

Within the Ste50-Ste11 complex, Ste11 is activated through interactions with Ste20/Cdc24/Cla4 and begins downstream regulation and osmoadaptive response through Hog1 interaction. Activated Ste11 proteins contribute to cell growth (Lee and Elion 1999; Liu et al. 2017). The greater abundances of Sho1, Cdc24, Cla4, Ste50, and Ste11 in the slow-growing,

high-ED_{50} DS 0982 isolate and their relatively lower abundances in the fast-growing, low-ED_{50} DS 1091 provide further confirmation of the inverse trend in HOG pathway response in the two isolates when experiencing salt stress.

Following Ste11 activation, through collaboration with the Ste50-Ste11 complex and recruitment of Ste11 activators Ste20/Cla4/Cdc24 via the Cdc42-Ste20 kinase complex, the Ste11-Ste50 complex binds via Ste50 to the cytoplasmic region of the membrane-anchored Sho1 (Gu et al. 2014; Wang et al. 2021). Sho1 recruits inactivated Pbs2 and activated Ste11, via the Ste11-Ste50 complex, in order to facilitate indirect docking and activation of Pbs2 by Ste11. Pbs2 appears a critical HOG pathway activator regulated in initiation and subsequent activity by both the Sln1 and the Sho1 branches through a TCS phosphorelay. Pbs2 activation via the Sho1 branch results in pathway activation and subsequent adaptive facilitation by adapter proteins Cdc42, Ste50, and Sho1 respectively (Tatebayashi et al. 2006; 2020).

While Pbs2 acts to activate Hog1 proteins in order to initiate subsequent adaptive responses, Ptp2/3 proteins work in a Hog1-dependent, negative feedback loop to dephosphorylate and deactivate activated Hog1 proteins (Jacoby et al. 1997; Hohman et al. 2007; Muakami et al. 2008; Liu et al. 2020). Along with the Ptp2/3 negative regulator proteins, another negative regulator, Ptc1, also works to deactivate HOG activity through indirect dephosphorylation of Pbs2 and direct dephosphorylation of Hog1 (Warmka et al. 2001; Lemos et al. 2018). These groups of negative regulators target Hog1 dephosphorylation differently: Ptc1 acts to dephosphorylate phosphothreonine likely within the cytoplasm, whereas Ptp2/3 act to dephosphorylate phosphotyrosine, possibly in either the cytoplasm or the nucleus (Homann 2009). These negative HOG pathway regulators, Ptp2/3 and Ptc1, induce expression in response to osmotic stressors in a Hog1-dependent manner (Jacoby et al. 1997). While Ptc1 abundance

relatively decreased in response to salinity across isolates – indicating a potential positive effect on Hog1 activation kinetics leading to an implied increased abundance of activated Hog1 within the cytoplasm and subsequent nuclear transport of activated Hog1 – Ptp2/3 proteins increased in abundance in response to salinity across isolates, likely demonstrating a negative regulation of Hog1 and increased effort to inactivate Hog1 – effectively replenishing the inactivated Hog1 stock in the cytosol (Fig 6).

Even with a greater abundance of upstream regulators, Hog1 seemed resistant to salinity and was unresponsive in the DS 0982 isolate, whereas its abundance decreased in response to salinity in DS 1091 (Fig. 6). Upon initiation by Pbs2, Hog1 proteins become activated and are transported from the cytoplasm to the nucleus where they induce expression resulting in adaptive response to osmotic stressors. The Hog1 transcriptional regulation increases glycerol production (Konte et al. 2016), activates glycerol symporter, Stl1, channels (Zemančíková et al. 2019), and closes Fps1 glycerol leak channels through phosphorylation activation of transcriptional factors (Lee et al. 2013). Although Hog1 abundances responded inconsistently across the two isolates, downstream Hog1 adaptive response instigators responded uniquely to prolonged salinity stress (Fig. 6).

We also observed differences in protein abundances that are associated with different aspects of the cell cycle. Cdc28, a Hog1 induced adaptive response regulatory protein, is a cyclic-dependent kinase (CDK) that regulates cell-cycle. Its greater abundance has been reported to correlate with a cell's ability to efficiently re-enter the cell-cycle post-stress (Nadal-Ribelles et al. 2014). In response to prolonged salinity, Cdc28 was downregulated in both isolates. Its lower abundance suggests that the isolates continue to experience stressors and remain unable to re-enter normal cell-cycle because of the prolonged salinity. Mcm1 mediates expression of a cell-

cycle regulator and CDK associate Cip1 (Chang et al. 2017). Functionally, Cip1 acts on CDKs associated with the G1 growth phase of the cell-cycle and inhibits cycle progression upon activation. During conditions consistent with osmotic stress, Hog1 phosphorylates and subsequently activates Msn2,4 which activates Mcm1 to trigger Cip1 and induce a secession in cell-cycle continuity (Chang et al. 2017). In response to salt, Mcm1 abundance increased dramatically in the slow-growing, high-ED_{50} DS 0982 isolate and a decreased in DS 1091 isolate. This suggests sustainable, conservative growth regulation in DS 0982 individuals and a relatively unchecked response in DS 1091 (Fig. 6).

Two downstream Hog1 transcriptional proteins, Tup1 and Ssn6, form a co-repressor complex that evidently regulates osmostress response by repressing expression of osmoadaptive genes (Márquez et al. 1998). The Tup1-Ssn6 complex is recruited to an active promoter and associates with a sequence-specific repressor to mediate an interaction with RNA polymerase II in order to halt transcription (Malavé and Dent 2006). Although these co-repressors act in unison as a complex to regulate transcription, their responses to persistent salinity differed between the isolates. Tup1 abundance increased in response to salinity in DS 0982 isolate, whereas it decreased in DS 1091 isolate. In contrast, Ssn6 protein abundance consistently decreased across the isolates in response to salt (Fig. 6).

Hog1 activity regulates the Cct1 translational effector whose expression is induced in response to osmotic stress (Herrero et al. 2008). Ctt1 encodes for a cytosolic catalase T, which protects glucose-6-phosphate dehydrogenase (G6PH) from stress-mediated inactivation (Lushchak and Gospodaryov 2005). Ctt1, through the encoded catalase T, is a critical antioxidant defense necessary for the degradation of reactive-oxygen species (ROS). ROS, through oxidation, inactivate G6PH and other ROS-sensitive enzymes and proteins.

G6PH plays an important role in the pentose phosphate pathway and is crucial for sustained energy production and redox response within fungal cells (Heinisch et al. 2020) as well as for providing upstream materials for glycolysis-mediated glycerol production (Fillinger et al. 2001). Further, G6PH actively reduces $NADP^+$ to NADPH to be used in many biosynthetic and detoxification responses (Levy 1979). NADPH is especially useful in the detoxification of ROS, which are major contributors to cellular oxidative stress (Breitenbach et al. 2015). In addition to detoxifying intracellular ROS, an increase in NADPH induces electron transport activity (Koshkin and Pick 1993), associates with the cell membrane to affect pH and impact electrochemical-driven ion fluxes and cell turgor (Segal 2016), as well as contributes to the accumulation and release of ROS to the extracellular space where they may take part in cell-wall modification, communication, and defense via signaling (Podgórska et al. 2017) – all of which would benefit osmoadaptation. While Ctt1 responses to salinity differed only nominally between the two conditions, with a slight increase in abundance in DS 1091 when experiencing salinity – it is notable that DS 1091 experiences greater abundance when compared to DS 0982 both with and without salinity induced response.

Ctt1 can be inferred to act as a cellular energy production regulator, may participate in general and oxidative stress response (Singh et al. 2021), and may be an anabolic response regulator (Wennekes et al. 1993). Ctt1 correlates most strongly with oxidative stress (Martínez-Pastor et al. 1996) and may be involved in assisting in cellular protection via reductive processing of ROS which accumulate in the cell during oxidative stress conditions. This strong correlation between Ctt1 and oxidative stress further support the notion that DS 1091 is experiencing markedly high levels of oxidative stress compared to DS 0982. Ctt1 abundance increased in our fast-growing, low-ED_{50} DS 1091 isolate in response to salt, whereas such

response was absent of minimal in the slow-growing, high-ED_{50} DS 0982 isolate. In correspondence with this, we infer that the slight upregulation of Ctt1 is likely to result from the aforementioned increase in inherent oxidative stressors experienced by DS 1091 isolates under the salt stress. Further, the lack of response of Ctt1 in the DS 0982 isolate reasons a relatively low inherent oxidative stress experienced by DS 0982 isolates when compared to DS 1091 isolates.

For DS 1091 this appears to indicate a greater need to combat ROS-inactivation which is possibly due to the faster growth of this isolate. Coupling this with the findings of decreased galactose metabolism and the implied resultant lower glycerol abundance of glycerol precursor biomolecule G6P in DS 1091 (cluster 2 of the KEGG Pathway analysis in Fig. 3), we suggest a potentially disruptive oxidative stress. This oxidation could inactivate G6PH enzymes, necessary for G6P to be converted into the necessary downstream molecules for glycerol biosynthesis. This further corroborates the lack of glycerol-mediated osmoadaptive responses in DS 1091 when compared to DS 0982 in response to prolonged salinity.

During osmotic stress, cells experience challenges ranging from ion toxicity, water loss, and cellular turgidity concerns. The HOG pathway attempts to alleviate these challenges by counteracting the gradient effects and achieves adaptive response through transcriptional regulations that ultimately aim to increase osmolyte accumulation, decrease osmolyte loss, and increase osmolyte production. The primary compatible solute produced to counter high osmolarity, glycerol, is produced via an increase in the downstream induced expression of the Gdp1 gene. Gpd1 encodes for glycerol-3-phosphate dehydrogenase (GDPH) and upon Hog1 induction increases production of GDPH enzymatic proteins (Albertyn et al. 1994). Consistent with the inverse trends among the two isolates, Gdp1 abundance decreased in DS 1091 in

response to salt, whereas Gdp1 abundance in DS 0982 it greatly increased. This is critical to HOG Pathway osmoadaptation with glycerol as the chief compatible osmolyte to combat salt stress. GDPH enzymes act on the glycolysis by-product dihydroxyacetone phosphate converting it into L-glycerol 3-phosphate. From here, a second enzyme is recruited to convert L-glycerol 3-phosphate into glycerol, the compatible osmolyte (Gencedo et al. 1968; Nevoigt and Stahl 1997). Glycerol accumulation combats the osmotic potential for permeating ions across the plasma membrane and restores cell functionality during stress (Plemenitaš et al. 2014).

Glycerol accumulation and regulation is also proposed to occur through membrane transporting proteins such as the glycerol symporter Stl1 (Ferreira et al. 2005) and the opening or closing of the glycerol transport channel Fps1 (Lee et al. 2013). Glycerol biosynthesis through MAPK signaling has been suggested the most crucial osmoadaptive response in fungal cells (Babazadeh et al. 2014). Understanding the salt responses via the HOG pathway permits a clearer understanding in the variability of salt-induced hyperosmotic adaptive stress responses among filamentous fungi in general and within *P. macrospinosa* in particular. However, our current understanding of cellular osmotic responses to salinity also highlights interactions with two other cellular targets for combating the associated stressors in fungal – the cell membrane and cell wall (Ene et al. 2015; Pérez-Llano et al. 2020).

References

Albertyn J, Hohmann S, Thevelein JM, Prior BA. 1994. GPD1, which encodes glycerol-3-phosphate dehydrogenase, is essential for growth under osmotic stress in *Saccharomyces cerevisiae*, and its expression is regulated by the high-osmolarity glycerol response pathway. Mol Cell Biol 1994; 14:4135–4144

Babazadeh R, Furukawa T, Hohmann S, Furukawa K. 2014. Rewiring yeast osmostress signalling through the MAPK network reveals essential and non-essential roles of Hog1 in osmoadaptation. Sci. Rep. 4:4697.

Bahn YS, Xue C, Idnurm A, Rutherford JC, Heitman J, Cardenas ME. 2007. Sensing the environment: lessons from fungi. Nat Rev Microbiol. 5:57-69.

Breitenbach M, Weber M, Rinnerthaler M, Karl T, Breitenbach-Koller L. 2015. Oxidative stress in fungi: its function in signal transduction, interaction with plant hosts, and lignocellulose degradation. Biomolecules. 5(2):318-342.

Carbó N and Pérez-Martín J. 2010. Activation of the Cell Wall Integrity Pathway Promotes Escape from G2 in the Fungus Ustilago maydis. PLoS Genet 6(7):e1001009.

Chang Y-N, Tseng S-N, Huang Y-C, Shen Z-J, Hsu P-H, Hsieh M-H, Yang C-W, Tognetti S, Canal B, Subirana L, Wang C-W, Chen H-T, Lin C-Y, Posas F, Teng S-C. 2017. Yeast Cip1 is activated by environmental stress to inhibit Cdk1–G1 cyclins via Mcm1 and Msn2/4. Nat Commun. 8:56.

Chen H, Zhou X, Ren B, Cheng L. 2020. The regulation of hyphae growth in *Candida albicans*. Virulence 11(1):337-348.

Correia I, Alonso-Monge R, Pla J. 2010. MAPK cell-cycle regulation in Saccharomyces cerevisiae and Candida albicans. Future Microbiol 5(7):1125-41.

Dexter JP, Xu P, Gunawardena J, McClean MN. 2015 Robust network structure of the Sln1-Ypd1-Ssk1 three-component phospho-relay prevents unintended activation of the HOG MAPK pathway in Saccharomyces cerevisiae. BMC Syst Biol. 9:17.

Dichtl K, Samantaray S, and Wagener J. 2016. Cell wall integrity signaling in human pathogenic fungi. Cellular Microbiology 18:1228– 1238.

Dihazi H, Kessler R, and Eschrich K. 2001. Phosphorylation and Inactivation of Yeast 6-Phosphofructo-2-kinase Contribute to the Regulation of Glycolysis under Hypotonic Stress. Biochemistry 40 (48):14669-14678.

Duran R, Cary JW, Calvo AM. 2010. Role of the osmotic stress regulatory pathway in morphogenesis and secondary metabolism in filamentous fungi. Toxins (Basel). 2(4):367-381.

Ferreira C, van Voorst F, Martins A, Neves L, Oliveira R, Kielland-Brandt MC, Lucas C, Brandt A. 2005. A member of the sugar transporter family, Stl1p is the glycerol/H+ symporter in *Saccharomyces cerevisiae*. Mol Biol Cell. 16(4):2068-2076.

Fillinger S, Ruijter G, Tamás M, Visser J, Thevelein J, d'Enfert C. 2001. Molecular and physiological characterization of the NAD-dependent glycerol 3-phosphate dehydrogenase in the filamentous fungus Aspergillus nidulans. Molecular microbiology. 39:145-157.

Gancedo C, Gancedo JM, Sols, A. 1968. Glycerol Metabolism in Yeasts. European Journal of Biochemistry. 5:165-172.

Gu Q, Chen Y, Liu Y, Zhang C, Ma Z. 2014. The transmembrane protein FgSho1 regulates fungal development and pathogenicity via the MAPK module Ste50-Ste11- Ste7 in Fusarium graminearum. New Phytol. 206:315-328

Hagiwara D, Sakamoto K, Abe K, Gomi K. 2016. Signaling pathways for stress responses and adaptation in Aspergillus species: stress biology in the post-genomic era. Biosci Biotechnol Biochem. 80:1667-1680.

Heinisch JJ, Knuesting J, Scheibe R. 2020. Investigation of Heterologously Expressed Glucose-6-Phosphate Dehydrogenase Genes in a Yeast zwf1 Deletion. Microorganisms. 8(4):546.

Herrero E, Ros J, Bellí G, Cabiscol E. 2008. Redox control and oxidative stress in yeast cells. Biochim Biophys Acta. 1780(11):1217-35.

Hohmann S, Krantz M, Nordlander B. 2007. Yeast osmoregulation. Methods Enzymol. 428:29-45.

Hohmann S. 2009. Control of high osmolarity signalling in the yeast Saccharomyces cerevisiae. FEBS Letters. 583(24):4025-4029.

Jacoby T, Flanagan H, Faykin A, Seto AG, Mattison C, Ota I. 1997. Two protein-tyrosine phosphatases inactivate the osmotic stress response pathway in yeast by targeting the mitogen-activated protein kinase, Hog1. J Biol Chem. 272(28):17749-17755.

Kanehisa M, Sato Y, Morishima K. 2016. BlastKOALA and GhostKOALA: KEGG Tools for Functional Characterization of Genome and Metagenome Sequences. J Mol Biol. 428(4):726-731.

Kayingo G, Wong B. 2005. The MAP kinase Hog1p differentially regulates stress-induced production and accumulation of glycerol and D-arabitol in Candida albicans. Microbiology 151(9):2987-2999.

Knapp DG, Németh JB, Barry K, Hainaut M, Henrissat B, Johnson J, Kuo A, Lim JHP, Lipzen A, Nolan M, Ohm RA, Tamás L, Grigoriev IV, Spatafora JW, Nagy LG, Kovács GM. 2018. Comparative genomics provides insights into the lifestyle and reveals functional heterogeneity of dark septate endophytic fungi. Sci Rep. 8(1):6321.

Koshkin V and Pick E. 1993. Generation of superoxide by purified and relipidated cytochrome b559 in the absence of cytosolic activators. FEBS Lett. 327(1):57-62.

Lee BN and Elion EA. 1999. The MAPKKK Ste11 regulates vegetative growth through a kinase cascade of shared signaling components. Proceedings of the National Academy of Sciences. 96(22):12679-12684.

Lee J, Reiter W, Dohnal I, Gregori C, Beese-Sims S, Kuchler K, Ammerer G, Levin DE. 2013. MAPK Hog1 closes the S. cerevisiae glycerol channel Fps1 by phosphorylating and displacing its positive regulators. Genes Dev. 27(23):2590-601.

Lee J, Reiter W, Dohnal I, Gregori C, Beese-Sims S, Kuchler K, Ammerer G, Levin DE. 2013. MAPK Hog1 closes the S. cerevisiae glycerol channel Fps1 by phosphorylating and displacing its positive regulators. Genes Dev. 27(23):2590-2601.

Lee J, Reiter W, Dohnal I, Gregori C, Beese-Sims S, Kuchler K, Ammerer G, Levin DE. 2013. MAPK Hog1 closes the *S. cerevisiae* glycerol channel Fps1 by phosphorylating and displacing its positive regulators. Genes Dev. 27(23):2590-2601.

Lee KT, Byun HJ, Jung KW, Hong J, Cheong E, Bahn YS. 2014. Distinct and redundant roles of protein tyrosine phosphatases Ptp1 and Ptp2 in governing the differentiation and pathogenicity of cryptococcus neoformans. Eukaryotic Cell 13:796–812.

Lemos P, Ruiz-Roldán C, Hera C. 2018. Role of the phosphatase Ptc1 in stress responses mediated by CWI and HOG pathways in Fusarium oxysporum. Fungal Genet Biol. 118:10-20.

Levy HR, Daouk GH, Katopes MA. 1979. Regulation of coenzyme utilization by the dual nucleotide-specific glucose 6-phosphate dehydrogenase from Leuconostoc mesenteroids. Arch Biochem Biophys. 198(2):406-13.

Liu X, Zhou Q, Guo Z, Liu Peng, Shen L, Chai N, Qian B, Cai Y, Wang W, Yin Z, Zhang H, Zheng X, Zhang Z. 2020. A self-balancing circuit centered on MoOsm1 kinase governs adaptive responses to host-derived ROS in Magnaporthe oryzae. eLife Sciences. 9:e61605.

Liu, J, Wang, ZK, and Feng, MG. 2017. Characterization of the Hog1 MAPK Pathway in the Entomopathogenic Fungus Beauveria Bassiana. Environmental Microbiology. 19(5):1808-1821.

Malavé TM and Dent SY. 2006. Transcriptional repression by Tup1-Ssn6. Biochem Cell Biol. 84(4):437-43.

Mandyam K, Jumpponen A. 2005. Seeking the elusive function of the root-colonising dark septate endophytic fungi. *Stud. Mycol.* 53:173–189.

Márquez JA, Pascual-Ahuir A, Proft M, Serrano R. 1998. The Ssn6-Tup1 repressor complex of Saccharomyces cerevisiae is involved in the osmotic induction of HOG-dependent and -independent genes. EMBO J. 17(9):2543-2553.

Martínez-Pastor MT, Marchler G, Schüller C, Marchler-Bauer A, Ruis H, Estruch F. 1996. The *Saccharomyces cerevisiae* zinc finger proteins Msn2p and Msn4p are required for transcriptional induction through the stress response element (STRE). EMBO J. 15(9):2227-2235.

Martínez-Soto D, Ruiz-Herrera J. 2017. Functional analysis of the MAPK pathways in fungi. Revista Iberoamericana de Micologia 34(4):11301406.

Murakami Y, Tatebayashi K, Saito H. 2008. Two adjacent docking sites in the yeast Hog1 mitogen-activated protein (MAP) kinase differentially interact with the Pbs2 MAP kinase kinase and the Ptp2 protein tyrosine phosphatase. Molecular and Cellular Biology 28:2481–2494.

Nadal-Ribelles M, Solé C, Xu Z, Steinmetz LM, de Nadal E, Posas F. 2014. Control of Cdc28 CDK1 by a stress-induced lncRNA. Mol Cell. 53(4):549-561

Nevoigt E and Stahl U. 1997. Osmoregulation and glycerol metabolism in the yeast Saccharomyces cerevisiae. FEMS Microbiol Rev. 21(3):231-41.

Plemenitaš A, Lenassi M, Konte T, Kejžar A, Zajc J, Gostinčar C, Gunde-Cimerman N. 2014. Adaptation to high salt concentrations in halotolerant/halophilic fungi: a molecular perspective. Frontiers in Microbiology. 5:199.

Podgórska A, Burian M, Szal B. 2017. Extra-Cellular But Extra-Ordinarily Important for Cells: Apoplastic Reactive Oxygen Species Metabolism. Front Plant Sci. 8:1353.

Posas F and Saito H. 1998. Activation of the yeast SSK2 MAP kinase kinase kinase by the SSK1 two-component response regulator. EMBO J. 17(5):1385-1394.

Posas F, Wurgler-Murphy SM, Maeda T, Witten EA, Thai TC, Saito H. 1996. Yeast HOG1 MAP Kinase Cascade Is Regulated by a Multistep Phosphorelay Mechanism in the SLN1–YPD1–SSK1 "Two-Component" Osmosensor. Cell. 86:865–875.

Posas, Francesc, and Haruo Saito. 1997. Osmotic activation of the HOG MAPK pathway via Ste11p MAPKKK: scaffold role of Pbs2p MAPKK. Science. 276(5319):1702.

Raitt DC, Posas F, Saito H. 2000. Yeast Cdc42 GTPase and Ste20 PAK-like kinase regulate Sho1-dependent activation of the Hog1 MAPK pathway. EMBO J. 19(17):4623-4631.

Ramezani-Rad M, Hollenberg CP, Lauber J, Wedler H, Griess E, Wagner C, Albermann K, Hani J, Piontek M, Dahlems U, Gellissen G. 2003. The Hansenula polymorpha (strain CBS4732) genome sequencing and analysis. FEMS Yeast Res. 4(2):207-215.

Ramezani-Rad M, Jansen G, Bühring F, Hollenberg CP. 1998. Ste50p is involved in regulating filamentous growth in the yeast Saccharomyces cerevisiae and associates with Ste11p. Mol Gen Genet. 259(1):29-38.

Román E, Correia I, Prieto D, Alonso R, and Pla, J. 2020. The HOG MAPK pathway in Candida albicans: more than an osmosensing pathway. International Microbiology 23(1):23-29.

Román E, Nombela, C, and Pla, J. 2005. The Sho1 Adaptor Protein Links Oxidative Stress to Morphogenesis and Cell Wall Biosynthesis in the Fungal Pathogen Candida Albicans. Molecular and Cellular Biology 25.23:10611-0627.

Segal AW. 2016. NADPH oxidases as electrochemical generators to produce ion fluxes and turgor in fungi, plants and humans. Open Biol. 6(5):160028.

Singh Y, Nair AM, Verma PK. 2021. Surviving the odds: From perception to survival of fungal phytopathogens under host-generated oxidative burst. Plant Communications. 2(3):100142.

Stojanovski K, Ferrar T, Benisty H, Uschner F, Delgado J, Jimenez J, Solé C, Nadal E, Klipp E, Posas F, Serrano L, Kiel C. 2017. Interaction Dynamics Determine Signaling and Output Pathway Responses. Cell Rep. 19(1):136-149.

Tatebayashi K, Yamamoto K, Tanaka K, Tomida T, Maruoka T, Kasukawa E, Saito H. 2006. Adaptor functions of Cdc42, Ste50, and Sho1 in the yeast osmoregulatory HOG MAPK pathway. EMBO J. 25(13):3033-3044.

Tatebayashi K, Yamamoto K, Tomida T, Nishimura A, Takayama T, Oyama M, Kozuka-Hata H, Adachi-Akahane S, Tokunaga Y, Saito H. 2020. Osmostress enhances activating phosphorylation of Hog1 MAP kinase by mono-phosphorylated Pbs2 MAP2K. EMBO Journal. 39:e103444.

Wang R, Ma P, Li C. 2019. Combining transcriptomics and metabolomics to reveal the underlying molecular mechanism of ergosterol biosynthesis during the fruiting process of *Flammulina velutipes*. *BMC Genomics* 20:999.

Wang X, Lu D, Tian C. 2021. Mitogen-activated protein kinase cascade CgSte50-Ste11-Ste7-Mk1 regulates infection-related morphogenesis in the poplar anthracnose fungus Colletotrichum gloeosporioides. Microbiological Research. 248:126748.

Warmka J, Hanneman J, Lee J, Amin D, Ota I. 2001. Ptc1, a type 2C Ser/Thr phosphatase, inactivates the HOG pathway by dephosphorylating the mitogen-activated protein kinase Hog1. Mol Cell Biol. 21(1):51-60.

Wennekes LM, Goosen T, van den Broek PJ, van den Broek HW. 1993. Purification and characterization of glucose-6-phosphate dehydrogenase from *Aspergillus niger* and *Aspergillus nidulans*. J Gen Microbiol. 139(11):2793-2800.

Zamith-Miranda D, Heyman HM, Cleare LG, Couvillion SP, Clair GC, Bredeweg EL, Gacser A, Nimrichter L, Nakayasu ES, Nosanchuk JD. 2019. Multi-omics signature of *Candida auris,* an emerging and multidrug- resistant pathogen. mSystems 4:e00257-19.

Zemančíková J, Papoušková K, Peréz-Torrado R, Querol A, Sychrová H. 2019. Stl1 transporter mediating the uptake of glycerol is not a weak point of Saccharomyces kudriavzevii's low osmotolerance. Lett Appl Microbiol. 68:81-86.

6. Conclusion

Studies described in this thesis focused on two main themes: first, whether conspecific strains of ascomycetes would be ecotypically adapted to either dry or mesic environments as measured by MAP; second, how do conspecific strains that differ in their NaCl tolerance and in their cellular responses to NaCl stress. In the course of these studies, we tested the following initial hypotheses: (1) ascomycete species differ in their growth response to salinity across species; (2) conspecific strains from drier sites have greater salt tolerance than those from more mesic sites. In an effort to further investigate the underlying mechanisms and differences in adaptive responses within species, we designed an experiment in which two *Periconia macrospinosa* conspecifics expressing the greatest variance in ED_{50} and originating from environments with varying precipitation were subjected to prolonged salinity stress prior to proteomic analysis. Inferring cellular responses from the proteomic analysis, we hypothesized that (3) conspecifics differing in ED_{50} will differ in their proteomic profiles; (4) colony growth (ED_{50}) will correlate to cell wall related protein abundances under salt stress (signaling cell wall modifications); (5) colony growth will correlate to plasma membrane related protein abundances under salt stress (signaling cell membrane alterations); (6) the MAPK signaling pathway will be an evident strategy for tolerating prolonged salinity amongst conspecifics (suggesting "compatible-solute" strategy); and (7) that conspecifics demonstrating a greater ED_{50} will demonstrate greater abundance of proteins involved in salt-tolerant strategies such as cell wall, plasma membrane, and MAPK-related proteins than their counterparts originating from more mesic sites.

There was no strong support for our first hypothesis. In rejection of our original hypothesis (1), there was no evidence for ecotypic adaptation in response to salinity among the

five species of filamentous ascomycetes (Fig. 1). Further, our second hypothesis (2) was also rejected due to inconsistent relative response within species in relation to site origin and salt tolerance measured by ED_{50}, evident *in P. macrospinosa* and *F. equiseti* results (Fig. 1). However, KEGG pathway investigation (Fig. 3) supported our third hypothesis (3) of differing responses to saline stress through a variety of responses between the two selected isolates. These analyses strongly suggested that the high-ED_{50}, slow growth isolate (DS 0982) and the low-ED_{50}, fast growth isolate (DS 1091) differed in their strategies in response to NaCl stress. Our proteomic results demonstrated numerous and strong pathway-level proteomic changes in response to salinity. These responses included overall changes in metabolism, changes indicating plasma membrane and cell wall modifications and changes in glycerol production via MAPK signaling enrichment evident in cluster 5 (Fig. 3), and elaborated on in Figure 6, in support of our third (3), fourth (4), fifth (5), and sixth hypotheses (6).

Changes witnessed in Figures 3 and 4 further support our fourth hypothesis (4) through inferred cell wall modifications. DS 0982 appeared to have the greatest positive abundance response to salinity, indicating a superior osmoadaptive strategy compared to the downregulation of DS 1091. Further, the inferred changes in plasma membrane composition support our fifth hypothesis (5) through the enrichment of fatty acid metabolism and steroid biosynthesis, distinct in clusters 2 and 3 respectively (Fig. 3) and further distinguished by differences in plasma membrane related protein abundances listed in Figure 5. In further support of our fifth hypothesis (5) – DS 1091 showed the greatest negative growth response to salinity (Fig. 2) and correlative plasma membrane related protein abundance downregulation (Fig. 5), while the nominally responsive DS 0982 (Fig. 2) demonstrated an increased abundance of membrane relative proteins

Investigations on the protein-level provided further support of our later hypotheses (3;4;5), especially for the more NaCl tolerant, high ED_{50} isolate DS 0982. When observing the cell wall relevant proteins, the two isolates distinctly differed in response to NaCl stress (Fig. 4). For example, DS 0982 upregulated chitin synthase, suggesting more abundant chitin synthesis and resultant cell wall reinforcement, coupled with downregulation of chitinase, a chitin degrading enzyme. This response is opposite to that of DS 1091, indicating a stark contrast in NaCl response strategies. Correlating this proteome information with the growth data - the slow growing DS 0982 isolate may be continually investing in self-preservation tactics, while the fast-growing DS 1091 may be shutting down regulative activities, providing partial support for our fourth hypothesis.

Further protein-level investigations demonstrated differing membrane-relevant protein responses to salinity between the two isolates (Fig. 5). For example, very-long-chain 3-oxoacyl-CoA reductase and elongation of fatty acids proteins, strong indicators of sphingolipid biosynthetic processing, were upregulated in DS 0982 and changed inconsistently in DS 1091 in response to NaCl stress. Likewise, evidence of changes in ergosterol biosynthesis, a key membrane component involved in membrane rigidity and osmo-regulative ion permeability, was ample in our protein-level investigations (Fig. 5). Hyperosmotic conditions, enabled by the external NaCl ion challenges, have been suggested to reduce membrane fluidity, a correlate of ion permeability, and increase membrane rigidity, likely through increased membrane sterol abundance (Los and Murata 2004). Evidence for ergosterol biosynthesis, inferring membrane sterol composition amendment, is demonstrated through observed abundance variations of ergosterol biosynthesis contributors: CDP-diacylglycerol synthase, sterol C-14 reductase-like protein, and sterol 24-C methyltransferase. While these proteins were upregulated in DS 0982 in

response to salt - DS 1091, the low ED_{50} and fast growth isolate, expressed a decreased abundance in these particular proteins, suggesting a relative downregulation in sterol biosynthetic processes. These findings are consistent with the observed rapid decline in growth in response to NaCl.

In addition to the observed cell wall and plasma membrane modifications, we observed evidence to suggest "compatible-solute" strategy (6) within *P. macrospinosa* isolate DS 0982 elucidated most successfully through protein-level and MAPK pathway mapping investigations (Fig. 6) providing evidence for the presence and role in osmolyte regulation by the HOG pathway in *P. macrospinosa*. Most notably, the two isolates differed in their responses to salinity: slow growing DS 0982 generally upregulated proteins in this pathway, whereas DS 1091 downregulated most proteins, consistent with systematic shutdown.

The major goal of the HOG pathway is to combat osmotic stress via the production of the compatible-solute, glycerol. It has been suggested that the most crucial osmoadaptive response in fungi occurs through MAPK-regulated glycerol biosynthesis (Babzadeh et al. 2014). To that end, the glycerol production initiating protein, Gdp1, activated by Hog1, is especially informative for osmoadaptive response. Consistent with the inverse response trend between the two isolates, Gdp1 abundance decreased in DS 1091 in response to salt whereas it increased in DS 0982 (Fig. 6). Through this, we posit DS 0982 has higher glycerol production capability and is likely actively counteracting osmotic stressors while DS 1091 either has met a growth capacity or responds by shutting down cellular metabolism. Incredibly, these findings support our seventh hypothesis (7) due to the inverse responses of the conspecifics based on salinity induction. While DS 1091 was initially expected to outperform DS 0982 due to its site origin being drier than that of DS 0982, we amended this stance upon reflection of the ED_{50} results. The proposed impact

and correlation between ED_{50} and osmoadaptive protein abundance proved correct as DS 0982 demonstrated a greater abundance of plasma membrane, cell wall, and MAPK HOG pathway related proteins compared to DS 1091 as well as demonstrated less dramatic growth inhibition in response to salinity.

Confirming the presence and understanding the role of the HOG pathway in response to salt stress provides a clearer understanding of the variability of salt-induced hyperosmotic adaptive stress responses within *P. macrospinosa.* However, current understanding of cellular osmotic response also highlights complex interactions and interconnected responses with two other cellular targets in fungal organisms for combating these stressors: the cell membrane and cell wall (Ene et al. 2015; Pérez-Llano et al. 2020). We confirm that our isolates responded to salt stress and exhibited distinct salt-response strategies. We also confirm a greater abundance of osmoadaptive proteins present in DS 0982, our isolate originating from a wetter climate, than that of its conspecific DS 1091, originating from a drier climate. We also confirm the critical importance of HOG pathway response in mediating osmostress and effective osmoadaptive response.

Understanding soil-inhabiting and root-associated fungi is critical to ecosystem health. Whether through providing nutrient cycling and ecosystem services, or direct interactions with hostplants, fungal impacts cannot be ignored. Through the effects of climate change, and decreased precipitation patterns soil salinization is a major threat to plant and animal health as well as the overall function of our natural world. This research aims to fill the gap in our knowledge on the impact of salinity toward root-associated fungi and their limits in salt-tolerance both within and across species. Further, this study aids in identifying varying

functional adaptations soil-dwelling fungi depend on for survival in response to salt stress in soil matrices.

References

Babazadeh R, Furukawa T, Hohmann S, Furukawa K. 2014. Rewiring yeast osmostress signalling through the MAPK network reveals essential and non-essential roles of Hog1 in osmoadaptation. Sci. Rep. 4:4697.

Ene IV, Walker LA, Schiavone M, Lee KK, Martin-Yken H, Dague E, Gow NAR, Munro CA, Brown AJ. 2015. Cell wall remodeling enzymes modulate fungal cell wall elasticity and osmotic stress resistance. mBio. 6(4):e00986.

Los DA and Murata N. 2004. Membrane fluidity and its roles in the perception of environmental signals. Biochim Biophys Acta. 1666(2):142-157.

Pérez-Llano Y, Rodríguez-Pupo EC, Druzhinina IS, Chenthamara K, Cai F, Gunde-Cimerman N, Zalar P, Gostinčar C, Kostanjšek R, Folch-Mallol JL, Batista-García RA, Sánchez-Carbente MdR. 2020. Stress Reshapes the Physiological Response of Halophile Fungi to Salinity. Cells. 9(3):525.